Paula Sofia Fonseca Nabais

Departamento de Conservação e Restauro

Mestrado em Conservação e Restauro

Spectroscopic characterization of natural dyes by their non-invasive identification on pre-Columbian codices: the Maya yellow

Dissertação para obtenção do Grau de Mestre em

Mestrado em Conservação e Restauro, especialização em Ciências da Conservação

Orientador: Doutora Costanza Miliani, CNR, Universidade de Perugia, Itália

Co-orientador: Doutor Aldo Romani, CNR, Universidade de Perugia, Itália

Júri:

Presidente: Professora Doutora Maria João Melo, DCR, Faculdade de Ciência e Tecnologia, UNL

Arguente: Doutora Solange Muralha, DCR, Faculdade de Ciência e Tecnologia, UNL

Julho de 2014

FACULDADE DE CIÊNCIAS E TECNOLOGIA
UNIVERSIDADE NOVA DE LISBOA

Paula Sofia Fonseca Nabais

Department of Conservation and Restoration
Master degree in Conservation and Restoration

Spectroscopic characterization of natural dyes by their non-invasive identification on pre-Columbian codices: the Maya yellow

Faculdade de Ciências e Tecnologia, Universidade
Nova de Lisboa, Dissertation for the Master degree in
Conservation and Restoration, specialisation in Conservation Science

Supervisor: Dr Costanza Miliani
Co-supervisor: Dr Aldo Romani

Juri:
President: Professora Doutora Maria João Melo, DCR, Faculdade de Ciência e Tecnologia, UNL

Examiner: Doutora Solange Muralha, DCR, Faculdade de Ciência e Tecnologia, UNL

Julho de 2014

Spectroscopic characterization of natural dyes by their non-invasive identification on pre-Columbian codices: the Maya yellow ©

Acknowledgements

I would like to thank first to professor Maria João Melo, who believing in my capabilities, got me a project in a foreign country to learn more with a great group of conservation scientists, allowing me to expand my horizons. Moreover, Italy was an experience I shall never forget. Besides learning a new language and connecting with so many different people, it made me grew in so many ways that I could not have grown in Portugal. Because of this opportunity I am certain I became a better person, but also, a better professional.

Secondly, I have to thank to the wonderful people that received me in Perugia. Being alone in a new country is not easy, especially while doing a master thesis and these people made it a little bit better. To Dr Costanza Miliani I owe the success of this project, because without all the help and attention provided it wouldn't have been possible. By supporting all my ideas, and following me throughout all the complications, she became someone I admire very much. Also, David Buti, who helped me through my first laboratory days, answered all my questions and work side by side with me throughout all the experiments, either they were successful or not. He was a pillar in this project for all the help, but most of all, the support he gave me. All the people in the MOLAB laboratory deserve my many thanks, for helping when I needed the most, or just to find a spatula. Most of all, thank you to Celeste, Francesca e Chiara, who helped me becoming a better professional by accompanying me while I was learning to work better with FT-IR, SERS and UV-Vis. Without them it would have been much harder.

Thirdly, thank you to all my friends, both the ones made in Italy, who enjoyed with me the wonderful pleasures of this country, but also to the ones left in Portugal. To these latter I must say that you brought a little bit of home every time you spoke to me. Besides all the distance, you made this journey with me and helped me in ways you cannot grasp.

Finally, but most importantly, I thank to my grandparents. Without them this project abroad would not have been possible. I thank to my father, for all the help, worries and beliefs he put in me, knowing I could do this. To João Lourenço I owe more than a thank you. You believed in me and supported me in so many ways I shall never forget. We made this adventure together and I could not have had it any other way.

To my mother, I owe everything. You endlessly supported me even when distance was hard, but you always knew I could do this. You allowed me to grow and became someone better. Because of this I truly hope I made you proud.

Abstract

Mesoamerican cultures had a strong tradition of written and pictorial manuscripts, called the codices. In studies already performed it was found the use of Maya Blue, made from a mixture of indigo and a clay called palygorskite, forming an incredibly stable material where the dye is trapped inside the nanotubes of the clay, after heating. However, a bigger challenge lies in the study of the yellows used, for these civilizations might have used this clay-dye mixture to produce their yellow colorants.

As a first step, it was possible to provide identification, by non-invasive methods, of two colorants (a flavonoid and a carotenoid). While the flavonoid absorbed between 368-379 nm, the carotenoid would absorb around 455 nm. A temperature study also conducted allowed to set 140ºC as the desirable temperature to heat the samples without degrading them. FT-IR, conventional Raman and SERS allowed us to understand the existence of a reaction between the dyes and the clays (palygorskite and kaolinite), however it is difficult to understand it in a molecular point of view.

As a second step, five species of Mexican dyes were selected on the basis of historical sources. The Maya yellow samples were produced adapting the recipe proposed by Reyes-Valerio, supporting the yellow dyes extracted from the dried plants on the clays, with addition of water, and then heated at 140ºC. It was found that the addition of water in palygorskite would increase the pH, hence deprotonating the molecules having a clear negative effect in the color.

A second recipe was developed, without the addition of water; however, it was found that the use of water based binders would still alter the color of the samples with palygorskite. In this case, kaolinite without heating yield better results as a Maya yellow hybrid.

It was found that the Maya chemistry might not have been the same for all the colors. The Mesoamericans might have found that different dyes could work better to their desires if matched with different clays.

It was noticeable that for a clear distinction between flavonoids and carotenoids the reflectance and emission studies suffice, but when clay is added, Raman techniques will perform better. For this reason, conventional Raman and SERS were employed in order to create a database for the Mesoamerican dyestuffs for a future identification.

Keywords: Maya blue, Maya yellow, dye-clay hybrids, pre-Columbian codices, flavonoids, carotenoids.

Resumo

As civilizações mesoamericanas tinham uma forte tradição de manuscritos escritos e pictóricos, denominados códices. Em estudos já realizados verificou-se a utilização de Azul Maia, feito a partir da mistura de índigo e uma argila denominada paligorsquite, formando um material extremamente estável, onde o corante está preso no interior dos nanotubos da argila, após aquecimento. No entanto, o grande desafio encontra-se no estudo dos amarelos utilizados, pois estas civilizações poderão ter utilizado este hibrido de argila-corante para produzir tons amarelos.

Como primeira fase, tornou-se possível a identificação, por meio de métodos não invasivos, de dois corantes (um flavonóide e um carotenóide). Enquanto o flavonóide absorve entre 368-379 nm, o carotenóide absorveria a cerca de 455 nm. Um estudo de temperatura realizado permitiu definir 140 º C como a temperatura desejável para aquecer as amostras sem causar degradação. Métodos como FT-IR, Raman convencional e SERS permitiram compreender a existência de uma reacção entre os corantes e a argila (paligorsquite e caulino), no entanto, é difícil compreendê-la de um ponto de vista molecular.

Como segunda fase, cinco espécies de corantes mexicanos foram seleccionadas com base em fontes históricas. As amostras de amarelo Maia foram produzidas adaptando a receita proposta por Reyes-Valerio, misturando os corantes amarelos extraídos das plantas secas com as argilas e a adição de água, seguido de aquecimento a 140 º C. Verificou-se que a adição de água em paligorsquite iria aumentar o pH, desprotonando as moléculas tendo um efeito negativo na cor. Uma segunda receita foi desenvolvida, sem a adição de água. No entanto, verificou-se que a utilização de ligantes à base de água iria alterar a color das amostras com paligorsquite. Neste caso, caulino, sem aquecimento, produziu melhores resultados como um híbrido amarelo Maia.

Verificou-se que não existia apenas uma receita-tipo para estes híbridos maias. Os mesoamericanos podem ter compreendido que diferentes corantes funcionariam melhor se combinado com diferentes argilas. Para distinguir entre flavonóides e carotenóides, os estudos efectuados com UV-vis serão suficientes, mas quando a argila é adicionada, as técnicas Raman irão ter uma performance melhor. Por esta razão, Raman convencional e SERS foram utilizados com o fim de criar uma base de dados para os corantes mesoamericanos, permitindo uma identificação futura.

Keywords: azul Maia, amarelo Maia, híbridos corante-argila, códices pré-colombianos, flavonóides, carotenóides.

Index of Contents

Index of Figures

Index of Tables

Chapter 1: Introduction

1.1. Pre –Columbian codices

For thousands of years, sophisticated civilizations prospered in what is now South and Central America and various cities were built by different civilizations, such as the Maya (300 B.C. – 900 A.D.) in Yucatán and Mexico, and the Aztecs (1325–1521 A.D.), in the Valley of Mexico [1].

As stated by Haude [1], the culture of these civilizations culminated in a strong tradition of written and pictorial manuscripts. The scribes had an important role in Aztec society, for they produced extensive manuscripts recording in images and logophonetic writing, religious, calendrical and astronomical information [2]. After the Spanish conquest of Mexico, many of these written books, the codices, were lost. However, some of them survived and were brought to Europe, as bizarre objects. Nowadays, around 15 of these codices rest in several universities and libraries around the world [3, 4]. These codices show considerable beauty, very different from that found on European illuminated manuscripts. Little is known about the colorants that were used in Mesoamerican codices; however, sources such as the Florentine Codex can be very valuable in understanding the tradition of painting. As understood by Wallert, a description from the Florentine Codex suggests the use of inorganic pigments ("…*grinds pigments*…") as well as organic dyes ("…*a painter who dissolves colours*") [2].

The analysis of these codices presented for many years a big challenge. The lack of non-invasive methodologies did not allow for proper analysis to be made without affecting the structural unity of the manuscripts. However, in the last few decades, several non-invasive analytical tools and methodologies were developed, and provided ways for a better characterization of the artwork materials, without damaging the manuscripts. Four codices have already been studied by the MOLAB facility of Eu-ARTECH and CHARISMA European project [5] (namely Codex Cospi [6], Codex Fejérváry Mayer, Codex Zouche-Nuttall and Codex Tro-Cortesianus [7]) and one other (Codex Colombinus [8]) by a group of investigators from the Universidad Nacional Autónoma de México.

These non-invasive in situ studies provided insight into many colorants used by the Pre-Colombians, and there are some differences of the materials used according to the origin of the various codices. In fact, it was found that cochineal was used for the red areas in all codices, except for the Codex Tro-Cortesianus, where it was identified the presence of hematite-based red. For the blue areas it was very clear the presence of Maya blue, a known dye composed of indigo precipitated on a clay base. In some codices the yellow was composed of orpiment. However, it was also found an unknown yellow dye precipitated in clay, similar to Maya blue specimens. The non-invasive methodology was very useful to understand the materials composing the codices and also, providing new questions about the unknown and unidentified dyes as well as organic-inorganic hybrids (see Annex 5).

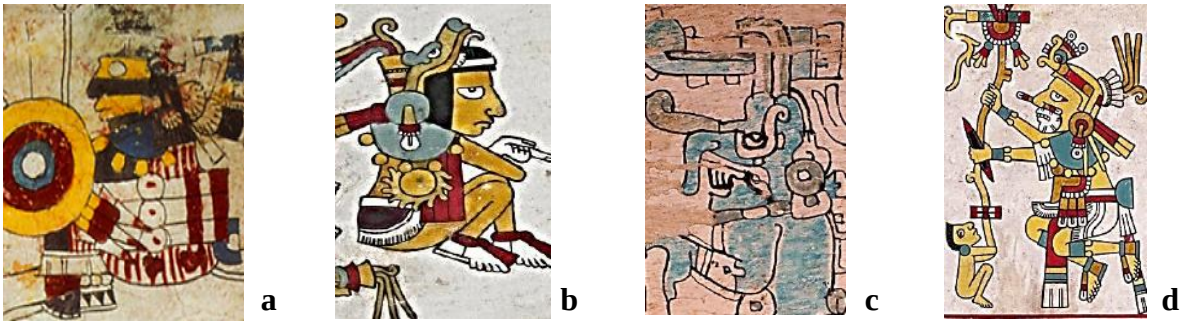

Fig. 1.1 – Details from different pre-Columbian codices studied by MOLAB: **a)** Codex Cospi, **b)** Codex Zouche-Nuttall, **c)** Codex Tro-Cortesianus, **d)** Codex Fejérváry Mayer.

1.2. Maya hybrid pigments

Very interesting was the use of dye-clay complexes to make very lasting paints. Such complex is very well known in the Maya blue. In fact, dye-clay complex of various colours such as yellow, red, blue and green have been identified in the Mayan mural painting tradition [3]. However, it was found that the usage of dyes was more similar to the textile industry than the mural painting [4].

1.2.1. "White earth"

Clays are nowadays widely applied in many fields due to their high specific surface area, chemical and mechanical stabilities, and a variety of surface and structural properties. Several clays, because of their unique structure have high binding affinities with various chemical species, such as organic molecules. Kaolinite and palygorskite are presented in this work as silicates capable of encapsulating such molecules.

Kaolinite, with the formula $Al_2Si_2O_5(OH)_4$, has crystals which are pseudo-hexagonal, along with plates, larger books, and vermicular stacks. However it has relatively low surface area in comparison to palygorskite [9, 10]. Fibrous clay minerals, such as palygorskite ($Si_8Mg_5O_{20}(OH)_2(H_2O)_4 \cdot 4H_2O$), have great potential for the retention of dyes, thanks to its high surface area [10]. Palygorskite is known as the clay in the Maya blue complex. The structure of this clay is based on a continuous tetrahedral sheet in which the SiO_4 tetrahedrons periodically (every two pyroxene-like chains) invert the orientation of their apical oxygen, which are bonded to z-elongated, discontinuous octahedral ribbons containing both magnesium and aluminum ions (Fig. 1.2).

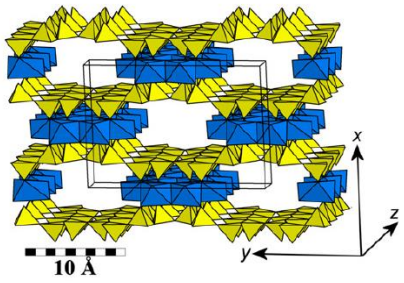

Fig. 1.2 - Structure of palygorskite. The microchannels are deprived of zeolitic water [11][1].

The structure is crossed by tunnels usually filled by weakly-bound zeolitic water molecules connected to the magnesium cations of the Mg (Al,Fe) ribbon edges of the channels [11, 12]. The palygorskite channels might be filled with water or organic molecules. In order for the organic molecule to be adsorbed, some water, such as the zeolitic water, must leave the palysgorekite structure.

1) Giustetto R. *et al.*, 2012, Microporous and Mesoporous Materials, No 155, pp. 167-176

This phenomenon happens with high temperature. In fact, it is proven that the heat from burning incense was one method to produce the Maya blue pigment [13]. It was found that dehydration of palygorskite takes place in a series of steps being the most important at approximately 120ºC with the loss of free pore water and water adsorbed on surface. The loss of both zeolitic and hygroscopic water occurs until 200°C [12].

1.2.2. The Maya blue

Produced in the Yucatán peninsula (Mexico) from the VII to XVI century A.D., the Maya blue pigment forms when the clay is mixed and heated (<200ºC) with the indigo dye [14]. Indigo (Fig. 1.3) is a natural blue dye formed by a mixture of coloring species of which indigotin is the primary species responsible for the distinctive blue color. The Mayas obtained indigo from a group of plants generically named *añil* or *xiuquitlitl* (mainly *Indigofera suffruticosa* (which the Mayans called *ch'ooh*)).

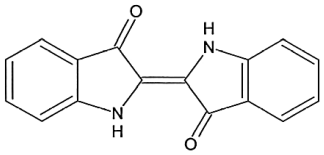

Fig. 1.3 – Chemical structure of indigo.

This compound can be considered an ancestor of modern hybrid materials, for an organic guest molecule is adsorbed within the pores of the hosting palygorskite frameworks [11].

The indigo in Maya blue is expected to diffuse, in some proposed models, inside the palygorskite tunnels and form specific host/guest interactions with the clay matrix. Encapsulation and bonding within the clay tunnels shield the dye molecules from external environment thus ensuring the pigment stability [11].

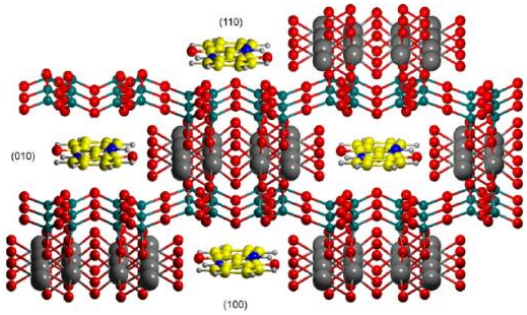

Fig. 1.4 - Structure of Maya blue. Indigo (yellow) is occupying both channels and grooves (H=white; C=yellow; N=blue; O=red; Si=light blue; Mg=gray) [15][2].

In 2008, Chiari G. *et al.*, presented a new model, in which the grooves (half channels, cut along their axis), were the main encapsulation sites for the indigo molecule (Fig. 1.4). Indigo cannot infiltrate the channels, since the formation of hydrogen bonds strongly binds the first molecule to the clay framework, preventing it from further penetration and impeding other molecules from entering [15].

Doménch A. *et al*. [16] found that the hue of the Maya blue is not just due to the indigo molecule, but is accompanied by other minority dyes which are distributed in different sites in the host palygorskite matrix, and different proportions of these components can give different hues. Also, because of its yellow color, dehydroindigo has been considered by many as a possible component to the formation of Maya yellow [16, 17].

2) Chiari G. *et al*., 2008, J. Paul Getty Trust, Applied Physics A, Materials Science & Processing, No 90, pp. 3-7

1.3. Maya hybrid pigments: the Maya yellow

For several years, scientists and historians thought they could understand the material with which the great civilizations of South and Central America made the color yellow. It was found in some codices the presence of orpiment and, although surprising, it was easily identified by Raman spectroscopy [3]. However, it was suggested by Vandenabeele *et al*. [18] that other pigments similar to Maya blue might exist. On mural paintings, Doménech *et al*. [19] reported the use of pigments similar in formation to Maya blue, and on codices as described before, it was found an emitting yellow dye precipitated onto a clay base, found through FTIR in reflection mode[3, 4, 6]. Therefore these evidences point out to the use of a yellow organic-inorganic hybrid pigment, besides Maya blue. It was found that, for Codex Cospi, several other organic-inorganic hybrids were used (light yellow, bright orangeish-yellow and orange) all composed by a mixture of a clay with an unknown yellow dye (found by UV-vis). On Codex Fejérváry-Mayer more dyes (red, orange and brown) were found to be mixed with clay, while on the Codex Colombinus the yellow dyes were not added to the latter. Also, to obtain an orange color, red and yellow dyes were mixed, while another orange was obtain by a single dye. This way is noticeable the plurality of different dyes, used to obtain different tonalities, which characterizes the different codices. In fact, sometimes it was found orpiment and no yellow dye at all (table A.12 of Annex 5) [3, 18].

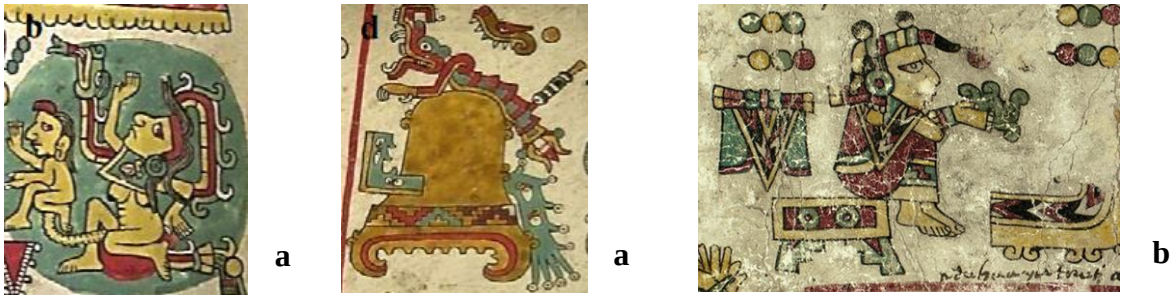

Fig. 1.5 – Yellow colored details from **a)** Codex Zouche-Nuttall and **b)** Codex Colombinus.

Buti did, in 2012, a series of studies comprising five species of Mexican dyes were selected both for their importance and availability in Mexico cultures [3]. Identification problems arose with the in situ study of Mesoamerican codices, suggesting the guidelines for the laboratory study and so Maya yellow pigments replicas were produced and characterized. Pure samples were preliminary investigated with HPLC-DAD in order to characterize the extract compounds from the selected plants (table 1.1). Afterwards, Raman, UV-vis reflectance and fluorescence spectroscopies were performed to highlight the characteristic spectral features of each dye and to investigate the clay-dye interaction occurring in the hybrid pigments. Furthermore, SERS technique was also applied only on pure dyes where conventional Raman appeared to be unsuitable due to the high fluorescence background.

Table 1.1 *- Identification of the main yellow and orange colours, with their Nahuatl names, European names, source and chemical components found by HPLC [3].*

***Nahuatl* name**	**European name**	**Botanical source**	**Chemical component**
Zacatlaxcalli	Barba de León	*Cuscuta* sp. *Cassytha* sp.	Quercetin, Kaempferol, Isorhamnetin
Xochipalli	Yellow Cosmos Orange Cosmos	*Cosmos sulphureus*	Luteolin-O-glucoside, Butein-O-glucoside, Luteolin, Quercetin, Butein
Achiotl	Annatto	*Bixa orellana*	Bixin, Crocetin
-	Pallo Amarillo Yellow fustic	*Cholophora tinctoria* *Maclura tinctoria*	Morin, Kaempferol
Zempoalxóchitl	Yellow Marigold Orange Marigold	*Tagetes erecta*	Quercetagetin-O-hexose, Quercetagetin, Patuletin

1.4. Objectives

This work intends to unveil the mysteries surrounding the Maya Yellow (MY), presenting a better understanding of this hybrid material, as well as to provide a database for yellow dyes not common in the European art history. For this, it is necessary to understand also the differences between some classes of colorants, such as the flavonoids and the carotenoids, present in plants that were most likely used to produce the yellow color in the Mesoamerican culture. This study tries to shed a light on their differences as colorants in the clay-dye hybrids, as well as the type of interaction they might have with the clay to understand how the Mesoamericans created such stable colorants. Also, since heating was used as an important step for the production of these hybrids, a detailed study on the effects of temperature on the molecules was performed.

Therefore, this study is separated in two parts:

- **The simplified Maya yellow replica**: where two basic colorants are used (a flavonoid and carotenoid) and mixed with two clays (palygorskite and kaolinite). This study intents to understand the dye-clay hybrid, has well as provide possible identification, by non-invasive methods, of flavonoids and carotenoids when mixed with clay.
- **The Maya yellow replica**: intents to complete the study performed in 2012 by Buti D., creating a database of Mesoamerican colorants, providing material for a good future identification of Maya yellows used in codices.

The application of a multi-technique approach is important for the characterization of the Maya yellow replicas. In fact, UV-vis absorption and fluorescence are methods easily applicable *in situ* and can provide information about the color properties of the materials. Also conventional Raman spectroscopy has a more precise molecular characterization with respect to fluorimetry, and it is use as a portable noninvasive instrument within MOLAB, as well as Fourier Transformed Infrared spectroscopy (FT-IR). Recent studies with Surface-enhanced Raman spectroscopy (SERS) active cellulose film that is removable from the surface prove that it will also be possible to use this technique as minimally invasive [20].

Chapter 2: Materials and Methods

Table 2.1 – *Table with the characterization of the methods and materials used.*

Replica	Materials	Recipe	Short name	Details
Simplified Maya yellow replica	Morin	Morin and Annatto were prepared at 20% in mixture with the two clays and several temperatures were employed from 140ºC to 220ºC.	MY simplified replicas	Percentage of dye set at 50% for annatto.
	Annatto			
	Clays: palygorskite and kaolinite			
Maya yellow replica	Fustic	1) Reyes –Valerio Recipe (dye + clay + water) 2) Modified Recipe (dye + clay)	MY replica	Percentage of dyes was set at 50%. Dyes were selected by their importance in Mexican culture and for their availability (see table 1.1)
	Orange Cosmos			
	Yellow Cosmos			
	Orange Marigold			
	Yellow Marigold			
	Zacatlaxcalli			
	Clays: palygorskite and kaolinite			

Analytical methods were performed, such as FT-IR, UV-Vis reflectance and emission, conventional Raman spectroscopy, as well as SERS. For more detailed about the methods used, please consult Annex 1.

Chapter 3: Results and Discussion

3.1. Spectroscopic characterization of simplified Maya yellow replicas: the morin and the annatto

The spectral characterization of simplified MY replicas is here reported and discussed. Because all the dyes at different extend showed a degradation at temperature higher than 140-160ºC (See the Temperature study in Annex 2) it was chosen to focus only the hybrid samples unheated and those heated at 140ºC.

3.1.1. UV-vis reflectance and emission spectroscopy

The UV-vis reflectance and emission spectra collected on simplified MY replica as powder are reported in figures 3.1-3.2 and compared with those of pure dyes and clays (See Annex 2 for the spectra and the tables with the absorption/emission maxima for all the samples). It's necessary to underline that all MY reflectance spectra are characterized by a sharp band in the near infrared region (at 1427 and 1404 nm for palygorskite and kaolinite respectively) assigned to the OH stretching combination bands (7280 and 7163 cm^{-1} for palygorskite and kaolinite respectively).

Morin MY's

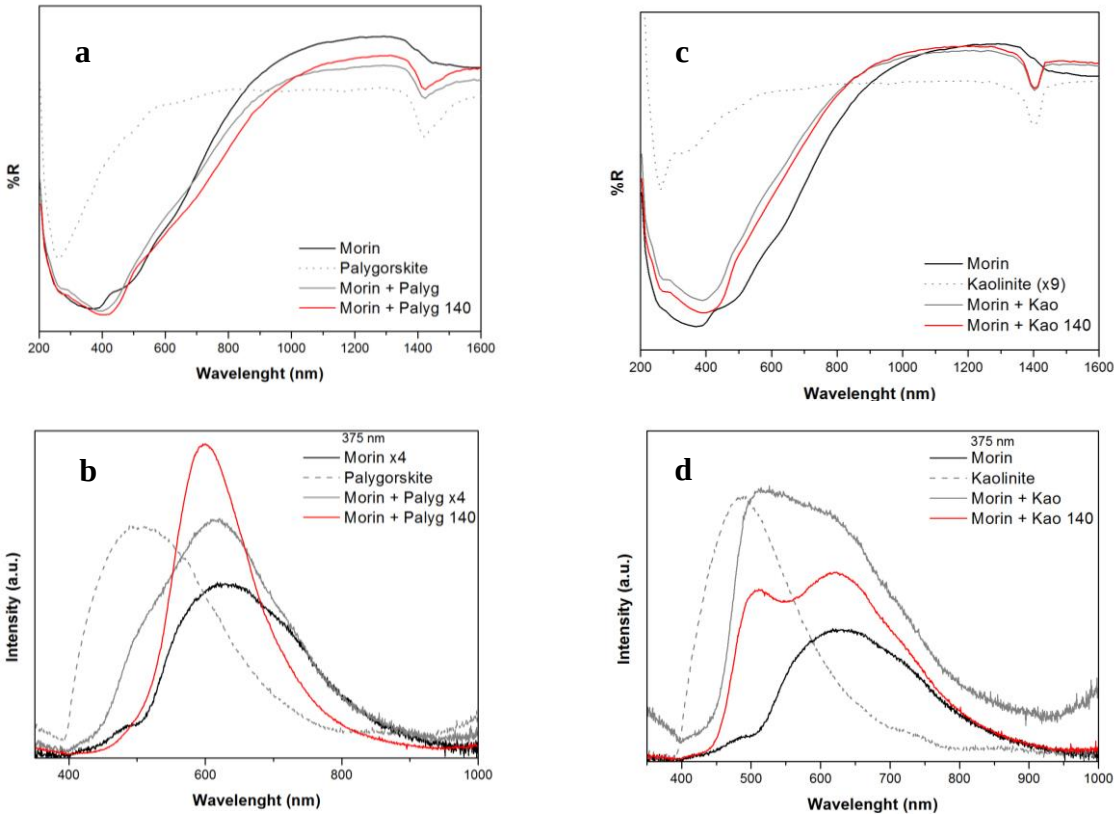

Fig. 3.1 – UV-vis spectral properties of morin MY's unheated and heated at 140ºC. Morin@palygorskite: a) reflectance and b) emission (λ_{exc}= 375 nm). Morin@kaolinite: a) reflectance and b) emission (λ_{exc}= 375 nm).

Morin is characterized by a band I and 368 nm and two shoulders at higher wavelengths. When kaolinite and palygorskite are added, the main band at 368 nm shifts to 400 nm indicating an

interaction of the hydroxyflavone with both clays. Differently from the thermal behavior of pure dye powder, for morin MY's it has barely no modification with increasingly higher temperatures, proving that the clays prevent thermal degradation.

Morin at the solid state exhibits a very low emission having a maximum at about 600 nm. It's important to report here that the emission of morin in solution is measured at circa 500 nm and is ascribed to a proton-transfer tautomer fluorescence band [21]. The emission spectra of the morin with the two clays give confirmation that some interaction takes place. The most evident effect is the quite important increase of emission intensity observed for both morin MY's with respect to pure morin. In particular, for morin@palygorskite excited at λ_{exc}= 375 nm, we see a hypsochromic shift, since the maxima go towards lower wavelengths (from 630 to 598 nm). For morin@kaolinite it is possible to see a creation of a double band (at 512 and 621 nm) in the spectrum, more evident in the heated sample. It is also very important to state the temperature stability that morin acquires when added to clay. In fact it remain very stable, because the maxima don't change abruptly until 180-200ºC, while the pure morin would only remain stable until 140-160ºC.

Annatto MY's

It is possible to see that there is almost no change or shifts in the reflection spectra.

Emission spectra recorded on the annatto MY's when compared with the spectrum of pure annatto in solid phase, suggest an interaction between carotenoid dyes and palygorskite. In fact, the maxima of emission bands of the specimens annatto@palygorskite both unheated and heated are blue shifted of c. 50 nm with respect to pure annatto. This shift is not occurring for the samples annatto@kaolinite. Also, the chlorophyll-*a* fluorescence emission spectrum is characterized by a major peak at 683 nm attributable to photosystem II which tends to decrease with higher temperatures.

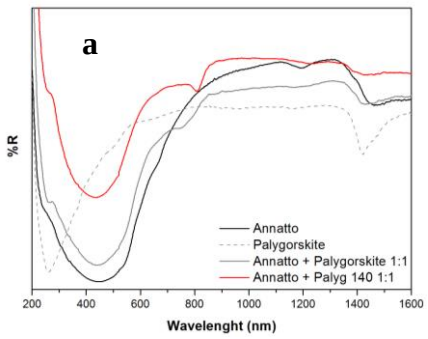

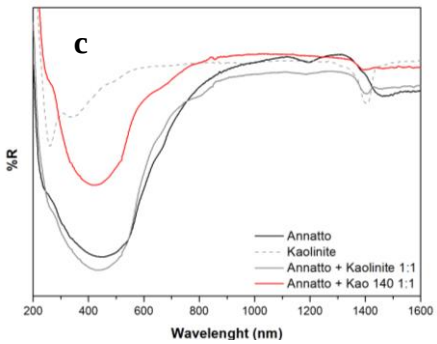

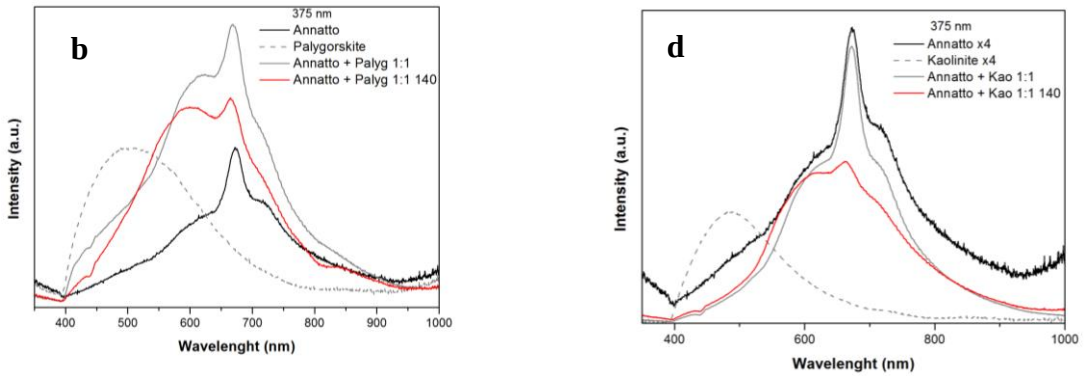

Fig. 3.2 – UV-vis spectral properties of annatto MY's unheated and heated at 140ºC. Annatto@palygorskite: a) reflection and b) emission (λ_{exc}= 375 nm). Annatto@kaolinite: a) reflection and b) emission (λ_{exc}= 375 nm).

3.1.2. FT-IR spectroscopy

The infrared spectra collected of the simplified MY replica, collected in transmission mode, are reported in Annex 2 (reference spectra of pure dyes and clays are also shown for comparison). In the morin-palygorskite spectrum, it is identifiable the bands corresponding to the clay: the 1191 cm^{-1} corresponds to the Si-O-Si bond between ribbons [22]. However, the peak at 1656 and 1606 cm^{-1} indicate the presence of morin, for they are related to the CC stretching of ring A and C, and to the C=O stretching of ring C, respectively. Also other peaks related to the morin molecule are presented in the morin-palygorskite hybrid, although with very small intensity. In the morin@kaolinite spectra, it can be seen the peaks corresponding to the clay, such as 1111, 1031 and 1007 cm^{-1} (Si-O stretching), but also 940 and 914 cm^{-1} (OH deformation of hydroxyl groups). However, it becomes very difficult to detect the dye when clay is added.

The spectra of annatto and both clays (20%) clearly show almost no presence of annatto, more specifically bixin, except for a small part in the higher wavenumber region. The region between 2000 and 1000 cm^{-1} should have several bixin bands if the molecule was present. However the presence of the bands in the 4000-2500 cm^{-1} region belonging to the hydrocarbon skeleton of bixin could indicate a small presence of the molecule, although not enough to produce a usable color. In fact Kohno Y. *et al*. [23] stated that the annatto did not adsorbed into motmorillonite by itself, and so, the samples were not colored, has it was found in this work. Because the FT-IR didn't present extensive results it was found unnecessary to perform these analyses in the 50% Annatto samples.

3.1.3. Conventional Raman spectroscopy

All the simplified MY samples were analyzed through conventional Raman. However, as stated before by Buti D. [3], while carotenoids presented characteristic scattering signals, the flavonoids show only a strong fluorescence background. As in this work, the extreme fluorescence of the morin molecule did not allow for conclusive results to be taken. For this matter, SERS was performed to the morin samples. Conventional Raman spectra of annatto MY's are reported in figure 3.3 and compared with that of pure annatto. Typical Raman bands of carotenoid structure are visible in

all the spectra, namely 1522, 1186, 1153 and 1005 cm^{-1} corresponding to the C=C stretching, CH bending and CC stretching and the CH3 bending of bixin, respectively [24]. It is important to underline that the scattering spectra did not shown any indication of a molecular interaction between annatto and the clays.

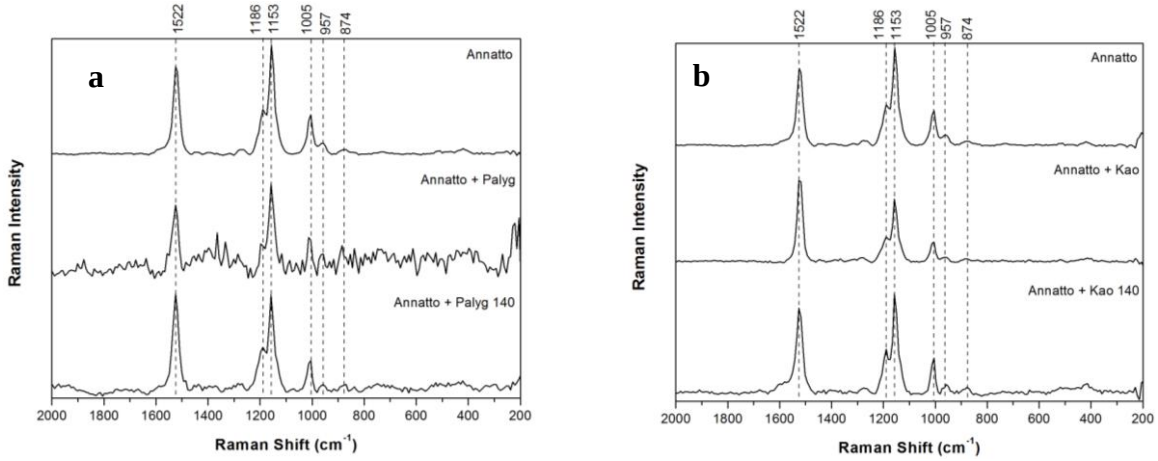

Fig. 3.3 – Normalized Raman spectra of a) annatto@palygorskite and b) annatto@kaolinite, (20% w/w), with heating at 140ºC (λ_{exc}=514).

The pure annatto degraded easily after 140ºC, as we see in the spectrum of the dye alone (Annex 2). However the clay might have sheltered the molecule until 180ºC. The Annatto at 50% was analyzed with λ_{exc}=785 nm and so the signal was too weak to represent.

3.1.4. SERS

In the SERS spectra of figure 3.4, representing the morin@clay hybrid it is possible to identify several peaks very similar to the ones found in the pure morin spectrum. The attemp of attribuition can be applied and several peaks such as 1639 and 1541 cm^{-1} can find similarities in the spectra already studied of morin (Annex 2). However it is possible to find some changes, such as in the area were it is likely related to the torsion of several CCCH bonds in the different rings (600-400 cm^{-1}). This could indicate a possible reaction with the clay. The '*' symbolizes the contribuition of the colloid.

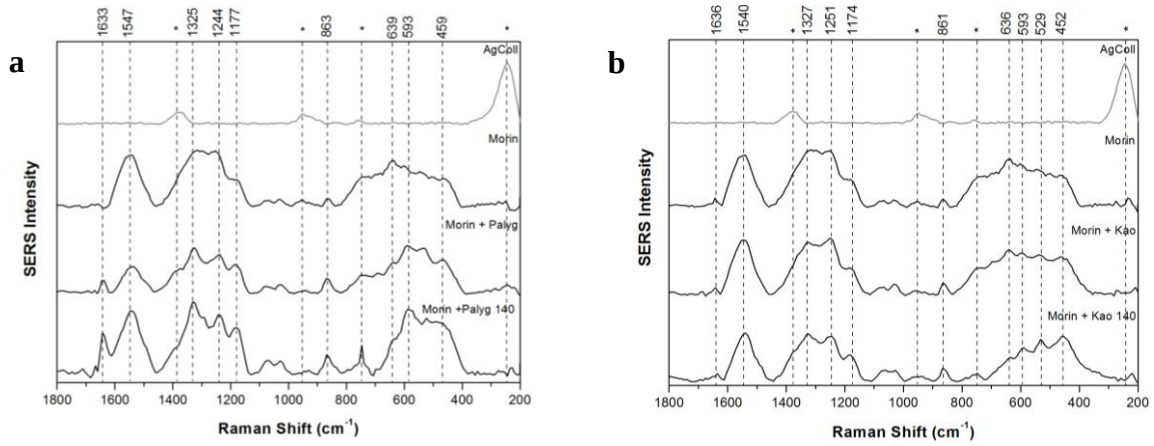

Fig. 3.4 – Normalized SERS spectra of a) morin@palygorskite and b) morin@kaolinite, with heating at 140ºC (λ_{exc}=514).

3.1.1. Discussion

As Buti D. [3], found, all the flavonoids show absorption maxima at 300-385 nm, and in fact here it was found that the morin absorbs between 368-379 nm. In fact, the UV–visible spectra of flavonoids are characterized by an intense Band I (here noticed at 368 nm) and diminished Band II absorptions (not visible in the reflectance spectra of morin) [25].

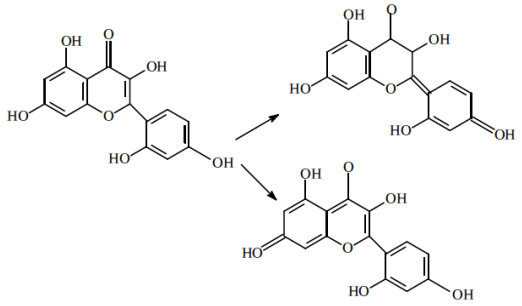

Fig. 3.5 - Illustration of the excited states of Morin [26][3].

In morin, these two band transitions are π-π* and can be represented by two ressonance structures (Fig. 3.5). The band at 368 nm suffers a bathochromic shift when clay is added to the morin samples, as well as the maxima at 424-494 nm. Also the emission spectra show that an interaction has taken place. In the morin@palygorskite spectra we see a hypsochromic shift while for morin@kaolinite we see a creation of a double band that becomes more evident with increasing temperature.

Also in the analyses of carotenoids, the UV-Vis spectroscopy is a valuable tool, because the absorption maxima, form, and fine structure of spectra are characteristic of the molecules chromophore [27]. Buti D. [3], found that most carotenoids absorb in the 433-500 nm region. In fact, these absorptions are found in the spectra above, but a bit shifted. It might have to do with the isomer in the powder – 9'-*cis*-bixin. This shift actually simplifies the distinction between flavonoids and carotenoids but not when the clays are added. Therefore this method might not be very reliable for this distinction, and other methods, such as vibrational techniques might show to be more useful.

The emission spectra of annatto@palygorskite show a possible interaction between the carotenoid and the clay, because the maxima of these species shifted 50 nm in relation to the pure annatto. The same does not occur for annatto@kaolinite.

The FT-IR presented some problems in understanding the possible reactions between the dyes and the clays. It was valuable for identifying between the dyes alone and also to characterize both clays. However when clay is added to the dyes it hides the signal from the latter. In this sense, Raman is presented as better tool because it picks up more effectively the dye, when using an excitation in the visible. SERS is necessary when dealing with flavonoids because of their strong fluorescence in Conventional Raman. With SERS some changes relating with both the morin and the morin@clay heated, were found, such as in the area were it is likely related to the torsion of several CCCH bonds in the different rings. This could indicate a possible reaction with the clay.

For the annatto dye, the conventional Raman method was in fact much more useful, since it was possible to see a better thermal stability of the molecule with the clays. In fact, bixin is considered to be unstable in the presence of heat, but some studies showed that the techniques of complexation and encapsulation decrease the degradation rate of bixin caused by high temperature [28]. This could

3) Wang F. *et al.*, 2012, Elsevier, Spectrochimica Acta Part A: Molecular and Biomolecular Spectroscopy, Nº 99, pp. 373-378

indicate that it is present a small, but existing reaction between the clay and the bixin. One hypothesis is that the bixin molecule is too long to fit in the inner channels of palygorskite, or between the plates and stacks of kaolinite. It might be a simple outer-surface reaction were the molecule sets in the grooves of palygorskite, or in the surface of the crystals of kaolinite, in such a small quantity that is not enough to color visibly the clay.

3.2. Maya yellow replica

3.2.1. Reyes-Valerio Method

The Reyes-Valerio method samples were first prepared by Buti D. [3] and then were further heated at higher temperatures (140ºC). These samples are prepared, has stated before, mixing the dyes (20% in weight) with the clay (kaolinite or palygorskite) while adding water. Images of the MY's replicas obtained following this method are shown in table 3.1.

It is clear that the heating followed by washing (see table 3.1) darkens the colors, specially those made with palygorskite. In fact, with heating at either 100ºC or 140ºC, the colors obtain with this clay are not similar to the real cases. Marigold is a clear example, where it acquires a green tone with palygorskite, but with kaolinite however, it shows a better tone, when it is heated at lower temperatures. Other dyes, such as cosmos or fustic, when heated at lower temperatures, present good similarities with the real cases of orange, but not yellow. Also zacatlaxcalli does not present, with palygorskite, a tone similar to the dye. It is clear, however, in zacatlaxcalli@kaolinite that the amount of dye is not sufficient. See Annex 2 for the UV-vis spectra of these samples.

Because of the intrinsic nature of some of these dyes to change color with the pH, it was found necessary to consider the effect of the clays on the pH of the solution containing the dyestuffs (see table 3.2 and 3.3). It was found that when water is added to palygorskite a pH of 8/9 is obtained, while for kaolinite only pH=6. For all of the pure dyes it was measured a pH=6, which with the addition of NaOH would increase to pH=7/8. The colors obtained were darker, with the exception of fustic, annatto and zacatlaxcalli.

Table 3.1 *– Photographs of the Maya yellow replica samples following the Reyes-Valerio recipe with heating at 100ºC and with heating at 140ºC (20% in weight of the dye).*

Samples	Heated at 100ºC			Heated at 140ºC		
	Dye	Dye @ Palygorskite	Dye @ Kaolinite	Dye	Dye @ Palygorskite	Dye @ Kaolinite
Fustic						
Orange Cosmos						
Yellow Cosmos						
Orange Marigold						
Yellow Marigold						
Zacatlaxcalli						

Table 3.2 *– Representation of the color and the pH of the pure dyes before addition of sodium hydroxide (NaOH) (with distilled water, pH=6) and after the addition of NaOH (pH=9).*

Compound	Before addition of NaOH		After addition of NaOH	
	pH	color of the solution	pH	color of the solution
Annatto[4]	6	transparent	7/8	yellow
Fustic	6	light orange	7/8	light orange
Orange Cosmos	6	orange	7/8	dark orange
Yellow Cosmos	6	light yellow	7/8	dark orange
Orange Marigold	6	light yellow	7/8	greenish yellow
Yellow Marigold	6	light yellow	7/8	greenish yellow
Zacatlaxcalli	6	transparent	7/8	yellow

4) Annatto is not found in the previous table because its characteristics are already described in Chapter 3.1. However, its pH sensibility was studied because it belongs to the 5 dyes chosen for this project.

Yellow marigold was chosen to perform the pH study because it was the dye that changed more when palygorskite and water were added (table 3.3). The measurement of pH with yellow marigold@palygorskite + water rendered a pH= 7/8, between the pH=6 of the dye and the pH=9 of the palygorskite. With kaolinite, the pH remains the same after the mixture. It is clear that the deprotonation of the molecules in a basic environment, caused by palygorskite, changes the color of the dyes (table 3.5 for main structures at different pH). A similar effect was found for alizarin with palygorskite which showed a remarkable red shift [14]. For these reason, this recipe does not presented good results for a MY replica. In fact, in table 3.4 it is possible to see that the addition of water, even without heating, clearly changes the color.

Table 3.3 *– Representation of the color and the pH measurements made to Yellow Marigold and the hybrid pigments with both clays (with water, pH=6).*

Sample	pH	Color
Yellow Marigold	6	light yellow
Palygorskite	8/9	white
Kaolinite	6	white
Yellow Marigold + Palygorskite	7/8	dark green
Yellow Marigold + Kaolinite	6	yellow

Table 3.4 *– Photographs of yellow marigold, comparing the effect of water in the color (see Annex 3 for the UV-vis and SERS spectra).*

Samples	Yellow Marigold@Palygorskite		
Without heating	Without Water	Prepared with water	Washed after preparation
			
Heated at 140ºC	Without washing	Washed	Reyes-Valerio Recipe washed
			

Table 3.5 *– Main structures found at pH= 6 and 9 for the various flavonoid compounds identified in the UV-Vis and SERS studies* (Chemicalize, ChemAxon, accessed May 2014, www.chemizalize.com).

	Main structures found at pH=6	**Main structures found at pH=9**
Morin	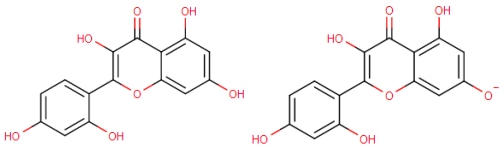	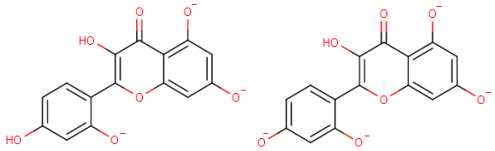
Luteolin	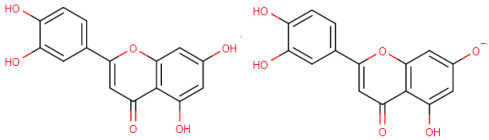	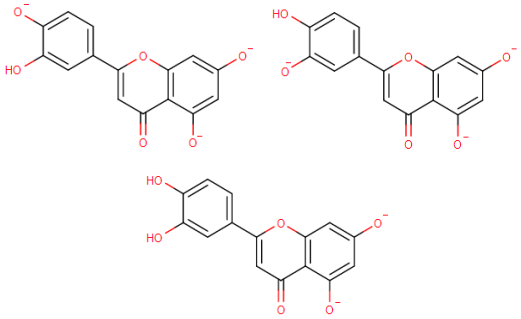
Butein	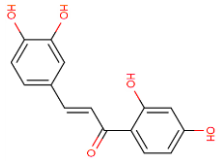	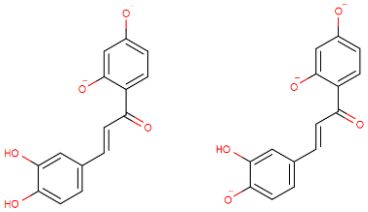
Patuletin	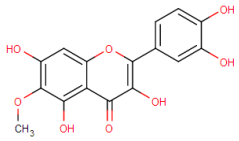	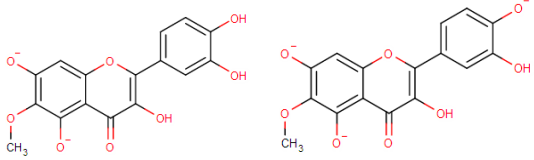
Quercetagetin	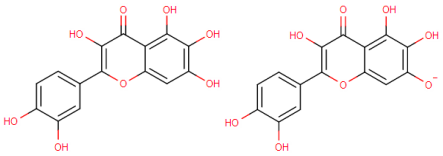	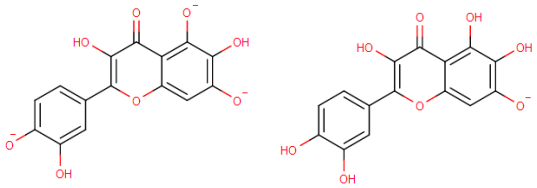
Bixin	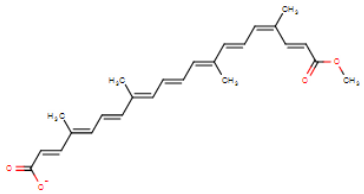	
Quercetin	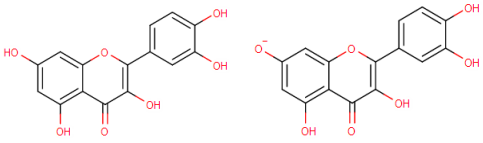	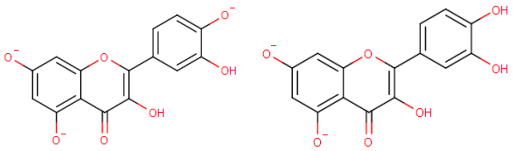

3.2.2. Modified Method

Since it was clear that the water causes the deprotonation of the molecules in the Reyes-Valerio method, some changes were employed such as not including water in the preparation and increasing the amount of dye to 50%.

Table 3.6 *– Photographs of the Maya yellow replica samples following the modified recipe, with and without heating at 140ºC (50% dye).*

Samples	Without heating		Heated at 140ºC	
	Dye@Palygorskite	Dye@Kaolinite	Dye@Palygorskite	Dye@Kaolinite
Fustic				
Orange Cosmos				
Yellow Cosmos				
Orange Marigold				
Yellow Marigold				
Zacatlaxcalli				

It is possible to see by table 3.6 that the removal of water in the preparation of the hybrid causes a positive effect. In fact, not only Marigold presents a better tone, but even Yellow Cosmos appears as a possible Maya yellow hybrid. However, it is noticeable the small darkening of the samples when heated, especially those with palygorskite.

A test was performed to better understand the effect of water based binders in the samples (these were found in all the codices – see Annex 5) by washing all the heated samples: the darkening of the color worsened as expected. Doménech-Carbó A. *et al.* [29] studying MY replicas similar to those here reported, found that upon the interaction with the clay, the flavonoid dye is accompanied by oxidation products.

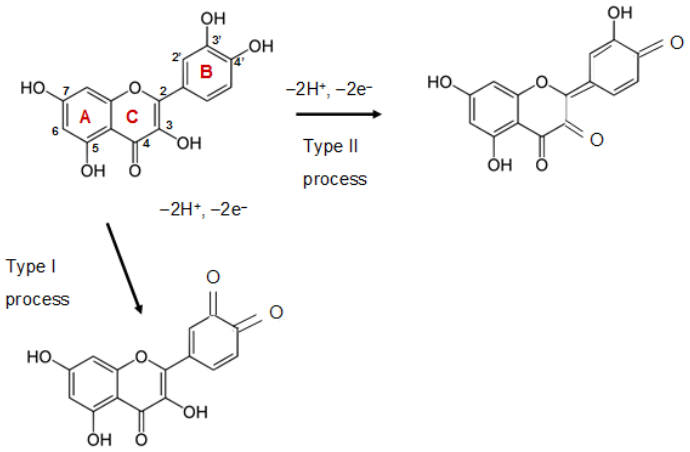

Fig. 3.6 – Quercetin molecule following type I oxidation or type II [29][5].

In particular, the authors found that the flavonoids containing two OH groups in the B ring would suffer a two-electron, two-proton oxidation (Type I), which occurs for quercetin, luteolin, butein, patuletin and quercetagetin. However, this process could be accompanied by the oxidation of one of the OH groups of the B ring and the OH of the C3 carbon in the ring C (Type II), which occurs for morin, isoharmnetin and kaempferol. They found that thermal treatment above 100ºC was the key, promoting the redox tuning accompanying the penetration of the dye in the palygorskite structure by linkage of the ring B to the clay channels.

It might be possible to consider that the heating promotes the creation of these oxidized species that may be water sensitive, altering greatly the color of the samples. In this case, kaolinite without heating yield better results as a Maya yellow hybrid, because the pH of kaolinite is equal to the protonated species of dyes and so the water in non-heated samples would not alter the color. Palygorskite, however, because of its basic pH when water is added might not perform as kaolinite with these binders.

It is necessary to state also the clear change in color of the dye when the clays were added. Flavonoids are known for their possible chelation with metal ions. For these, there are three potential coordination sites: between 5-hydroxy and 4-carbonyl group, between 3-hydroxy and 4-carbonyl group and between 3', 4'-hydroxy group in B ring. Quercetin, for example, chelates metals via 3', 4'-hydroxy group in B ring by its hydroxyl groups and also morin can form complexes with several metals like copper (II) [30].

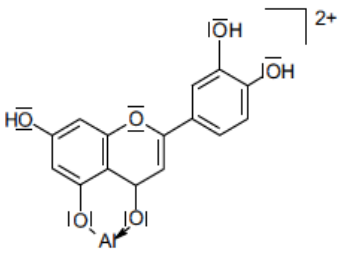

Fig 3.7 – Proposed structures of 1:1 luteolin-aluminum complexes [31][6].

Rygula A. *et al.*, found that luteolin connects with aluminum (III) by a conjugated system of an oxo group at C4 and a double bond at C2=C3. The complex is confirmed by the presence of 396 nm band in the UV–vis spectrum [31].

5) Doménech-Carbó A. *et al.*, 2014, Microporous and Mesoporous Materials, Nº 194, pp.135–145
6) Rygula A. *et al.*, 2013, Vibrational spectroscopy, Nº 64, pp. 21-26

3.2.2.1. UV-vis reflectance spectroscopy

The flavonoid molecules are known to be characterized in solution by two important absorptions: an intense Band I (300-390 nm) and a shorter Band II (220-270 nm) [3, 25]. In fact, with the exception of Annatto (already studied before), with its main component being a carotenoid, all of the other four botanic species (Fustic, Cosmos, Marigold and Zacatlaxcalli) are characterized by the presence of flavonoids and so, it is clear the presence of these two important bands in all the spectra (the band at 220-270 nm might be due to the low sensitivity of the detector at short wavelength). Also, the spectra of morin previously presented are easily compared to that of Fustic. There is a hipsochromic shift of these peaks related to those of morin, but this could be indicator of the presence of other species such as kaempferol.

Other important bands at 400-415 nm and 515-525 nm are described as Buti D. [3] as justifying the reddish and orange color of some speciemens. In fact these bands are only present in Fustic, Orange Cosmos and Zacatlaxcalli. These correlates the statement that the difference in color between Orange Cosmos and Yellow Cosmos is due to minor unidentified components, while the difference between Orange and Yellow Marigold might be due to different amounts of components.

Zacatlaxcalli is characterized by a main band at 400 nm which has not been identified. It does not coincide with any reflectance maxima of quercetin, kaempferol or isorhamnetin. Orange Cosmos presents small bands at 330 and 400 nm which can be attributed to the bands 324 and 399 nm of luteolin [32], visible also on the reflectance spectrum of Yellow Cosmos. Orange and Yellow Marigold both present a main peak at ≈375 nm that can be atribuited to patuletin. However, as Buti D. [3] found, both Marigold don't present the three main peaks at 430-470 nm of the carotenoid lutein, reported in literature as its main component. The addition of clay created a bathochromic shift of all the main peaks in all the dyes. See Annex 2 for the reflectance database created for the samples.

3.2.2.2. UV-vis emission spectroscopy

Chlorophyll is clearly present is some of the dyestuff similarly to Annatto. In fact, both Marigold and Zacatlaxcalli show a sharp emission around 680 nm (see Annex 2). It is important to state that Buti D. [3] didn't identify chlorophyll in any of the real case studies, but it is necessary to take into account its propensity to degrade.

Buti D. [3], found in his work that the dye + clay hybrids are characterized by a shift towards lower wavelengths in relation to the pure dyes. He also noticed this shift did not occur in the Annatto spectra. However, it is to be noted that a bigger shift occurs when the dye is mixed with palygorskite with respect to kaolinite. Also, Zacatlaxcalli presents a very small shift in regards to the other dyestuffs. With the modified method it is possible to see that only small shifts occurred when clay was added. Buti D. [3] stated that a possible chelation with a metal would shift the emission spectra to the red increasing the fluorescence emission. It is possible to notice this in some samples such as Fustic,

both Cosmos, Yellow Marigold and Zacatlaxcalli, but it is difficult to ascertain if a chelation does indeed occur. See Annex 2 for the emission spectra of the samples.

3.2.2.3. SERS

Since all the dyestuffs have flavonoids in their composition, the Conventional Raman spectra showed only fluorescence as expected. See Annex 2 for the SERS spectra.

SERS spectrum of Fustic is very similar to that of morin. In fact, even the band at 1644 cm^{-1} that appear in morin with palygorskite is present in Fustic with the same clay. It is to be noted that this band, however, is not present when the dye is added to kaolinite.

Orange and Yellow Cosmos do not present the characteristic bands of luteolin as expected, but instead show significant closeness to the bands report for quercetagetin, found in Marigold. The bands at ≈537, 732, 968 and 1327 cm^{-1} are reported in literature as belonging to this flavonoid [33]. The bands at ≈460, 400 and 333 cm^{-1} could be attribuited to butein. In fact, as showed by Buti D. [3], this flavonoid presents three small bands at 472, 407 and 339 cm^{-1}. In fact, the SERS spectra of both Cosmos could be a mixture of characteristic vibrations from these flavonoids. When the clays are added there is a decrease of intensity of the band at 732 cm^{-1}.

Both Orange and Yellow Marigold present bands correspondent to quercetagetin. According to Casanova-González E. *et al*. [33], the main dye of *Tagetes erecta* (Marigold) is quercetagetin, and it is possible to find similarities between the SERS spectrum of this study and the present one. In the low wavenumber range it is possible to find an intense band at 732 cm^{-1}, with more intense bands at 537 and 633 cm^{-1}. In the high wavenumber range we find bands at 1132, 1329, 1462 and 1609 cm^{-1}. The attribution of these bands to vibrational characteristics is still to be made. In the contrary to that of Cosmos, the band at 732 cm^{-1} does not decrease with the addition of clay.

SERS spectrum of Zacatlaxcalli is very similar to SERS spectrum of quercetin, as stated by Buti D. [3]. Also Casanova-González E. *et al* [33] found while studying Mexican dyestuffs, including Zacatlaxcalli, that the SERS spectrum corresponded to that of quercetin. The band at 417 cm^{-1} is related to the OH bending on ring C, and at 480 cm^{-1} there is the in-plane rotation of ring B and also an OH bending of ring C, while at 590 cm^{-1} there is the in-plane deformation of rings A and B, which is also represented by the band at 732 cm^{-1}. The bands at 1257 and 1457 cm^{-1} represent an OH, CH in-plane bending, while the band at 1507 cm^{-1} represents only a CH bending in ring B. Finally, at 1601 cm^{-1} there is the C=O stretching [34]. Very interesting is the differences between the spectra when a clay is added to the dye. In fact, there is a shift of the band at 480 cm^{-1}, but more importantly, the band at 732 cm^{-1} completely disappears.

3.2.3. Discussion

The UV-Vis reflectance and emission studies conducted allowed a better understanding of both the dyes alone but also the dye-clay hybrids. Indeed, it was possible to observe that the effect of

water in the Reyes-Valerio method has a negative role in the changes in color and shifts in the spectra observed. In fact, in this method, the red shifts of the spectra were visible immediately after adding the clays, and were more notable with palygorskite. This was found to be a problem related to a pH effect. In fact, flavonoids are known to have acidochromic properties.

Some of the compounds found in this work have already been studied in regards to their dependence on pH. Tungjai M. *et al*. [35] found that in acidic solutions the flavonoid kaempferol has an absorption band between 250 nm to 450 nm with the maximum absorbance at 363 nm, similar to that found by Buti D. [3]. When the pH of solutions was increased, they found that the peak was shifted toward the red end of the spectrum. Jurasekova Z. *et al*. [36] studied the effect of pH in various flavonoids and found that the UV-Vis spectrum of luteolin showed that a molecular deprotonation occurs. While with low pH there is an intense band at 345 nm, with increasingly higher pH this band decreases and a new band appears at 400 nm. Quercetin was reported to undergo several structural changes under alkaline conditions. This red shift is attributed to the deprotonation of OH groups in the B-ring. In SERS, these alterations are seen in the range of 500-400 cm^{-1}. The bands characteristic of quercetin, at 480 and 417 cm^{-1} tend to shift with higher pH [36].

This change in pH is responsible for the change in color of the samples. Therefore, it is possible to state that the protonation of the molecule has a very important role in these organic-inorganic hybrids. It is possible to admit that there is not only the original molecule, but various molecules with different states of deprotonation, depending on the pH (table 3.5).

The spectroscopic methods used were useful to distinguish between dyes, e.g. SERS, where it was found that the flavonoids present bands preferentially in the spectral ranges of 1600-1200 and 600-400 cm^{-1}. The band at 700-800 cm^{-1} seems to appear in all of the spectra as a characteristically vibration of flavonoids: in-plane C–C deformations of rings A and B.

Buti D., in 2012 [3], identified several components by HPLC-DAD which are represented in table 1.1. During his studies with conventional Raman and SERS, however, he found other species, namely a carotenoid (lutein), present in Marigold, not identified by HPLC. In the present study it was not possible to find lutein either by UV-Vis or conventional Raman. The excitation used in the Raman experiment (785 nm) was not the indicated one to identify carotenoids and in this case, the fluorescence of the other flavonoid components would mask the bands of lutein.

Even more interesting is the behavior of Zacatlaxcalli. Its behavior concerning the UV-vis studies, which had little changes even when washed, could be interpreted as usual characteristic of a carotenoid. The impediments of the methods stated before prevented it from being identified, but it is color resistant in comparison to the other dyestuff, which is indicative that the main chromophore might not be a flavonoid. In fact, Wallert *et al*. [2] stated that several of such compounds are present in Zacatlaxcalli, such as α/β/ϒ-carotene, lutein and esterified xanthophyll.

***Table 3.7** – Summary of what was found in this work through the spectroscopic methods employed.*

Dye		Spectroscopic study		Recipe	
		UV-Vis	**SERS and Raman**	**Reyes-Valerio**	**Modified**
Zacatlaxcalli		carotenoid?	quercetin	negative effect in the changes in color and shifts in the spectra due to a pH effect with palygorskite.	no changes in color if water is not added. With palygorskite, heating and water-based binders have a negative role.
Cosmos	**Orange**	luteolin	quercetagetin butein		
	Yellow				
Annatto		bixin	bixin		
Fustic		morin	morin		
Marigold	**Orange**	patuletin	quercetagetin		
	Yellow				
Conclusion		Palygorskite is not the ideal clay for a MY replica if these dyes are used. In fact, Kaolinite presented the best results even with water-based binders.			

3.3. Analysis of the codices

The MOLAB team was able to study three codices conserved in the Apostolic Library of the Vatican (Rome) and belonging to the Borgia group: Codex Borgia, Vaticanus A and B. The in-situ measurements allowed for a better understanding of these beautifull manuscripts. Because the aim of this work is the understanding of the Maya yellow hybrid, it was decided to represent only the data from the yellow measurements.

***Table 3.8** – Physical and historical characteristic of the three codices studied in the Vatican library.*

Codices	Borgia	Vaticanus A (3738)	Vaticanus B (3773)
Provenance	Probably from the centre of Cholula in the Puebla-Tlaxcala region, XV-XVI century	Probably painted in 1562, being copied from the Telleriano Remensis	Probably from the Puebla-Tlaxcala region, XV-XVI century
Contents	Ritual-divinatory book	Vary from mythological to calendrical.	Ritual-divinatory book
Characteristics	Typical pre-Columbian codex, composed of 16 pieces of animal skin joined to form a whole strip.	Colonial, large in-folio book, composed of 102 folios of European paper	Typical pre-Columbian codex, composed of 10 pieces of animal skin joined to form a whole strip.
Preparation	Composed of several white layers	White ground layer	
Drawing	Preparatory drawing		
Painting	All pages were painted both sides, except for the first and last, left blank	Most of the pages are painted and contain a lentthy italian text	All pages were painted both sides, except for the first and last, left blank

Methodology and spectroscopic characterisation of the codices:

All the codices were analysed by portable instruments such as Mid-Infrared spectroscopy (MIR), conventional Raman, UV-vis spectroscopy and X-ray fluorescence (XRF).

Fig 3.8 – MIR measurements of Codex Borgia

Codex Borgia: Preparation layer composed of gypsum and calcium carbonate. Several of the yellow/orange areas analysed are characterised by such a strong signal from the preparation layer, becoming difficult and sometimes impossible to distinguish any other component by MIR. However, for other areas, inverted bands at around 950, 980 and 1000-1010 cm^{-1} appeared, indicanting the possible presence of a clay. For the blue areas, the two most intense bands at 1033 and 980 cm^{-1} corresponding to the stretching mode of the Si-O bond of palygorskite, were successfully identified, probably indicating that this is not the clay present in the yellow areas, or it would have been identified.

Codex Vaticanus A: This colonial codex is characterised by the presence of several interventions and repaintings, which makes it difficult to analyse the original materials. In fact, for the yellow areas it was found tin (Sn) with XRF, malachite was found by MIR in the green areas and even Prussian blue and azurite were identified in the blue areas.

Fig 3.9 – XRF measurements of Codex Vaticanus A.

Fig 3.10 – UV-vis measurements of Codex Vaticanus B.

Codex Vaticanus B: Original preparation layer composed of calcium carbonate and kaolinite; repainted preparation layer composed of aragonite. A protein component was found which could indicate the presence of a protenaicious binder. Similar to codex Vaticanus A, some areas were repainted, which was indicated for the presence of other materials, such as Prussian blue.

Also, arsenic (As) was found by XRF in some yellow areas which could indicate the use of orpiment.

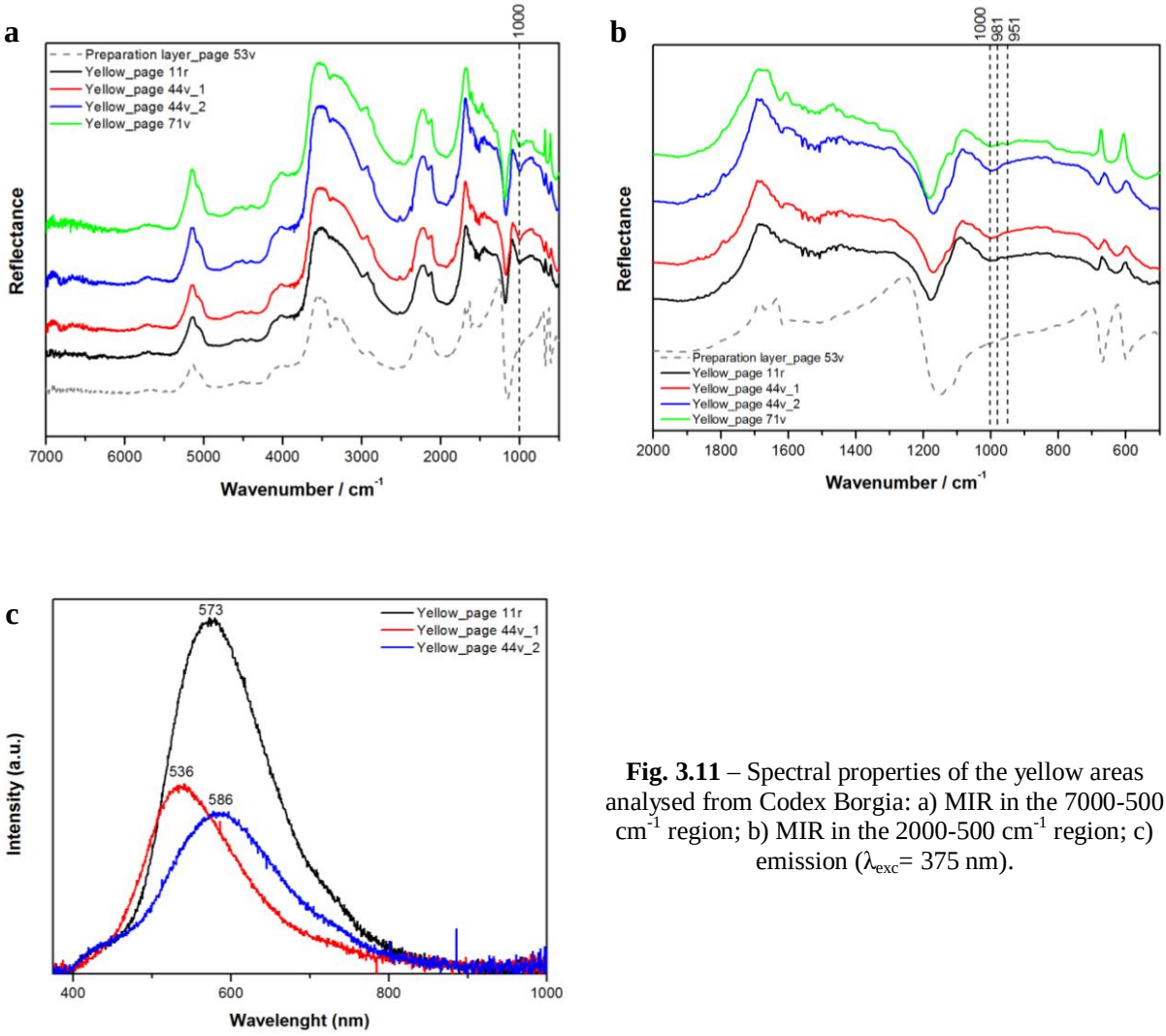

Fig. 3.11 – Spectral properties of the yellow areas analysed from Codex Borgia: a) MIR in the 7000-500 cm^{-1} region; b) MIR in the 2000-500 cm^{-1} region; c) emission (λ_{exc}= 375 nm).

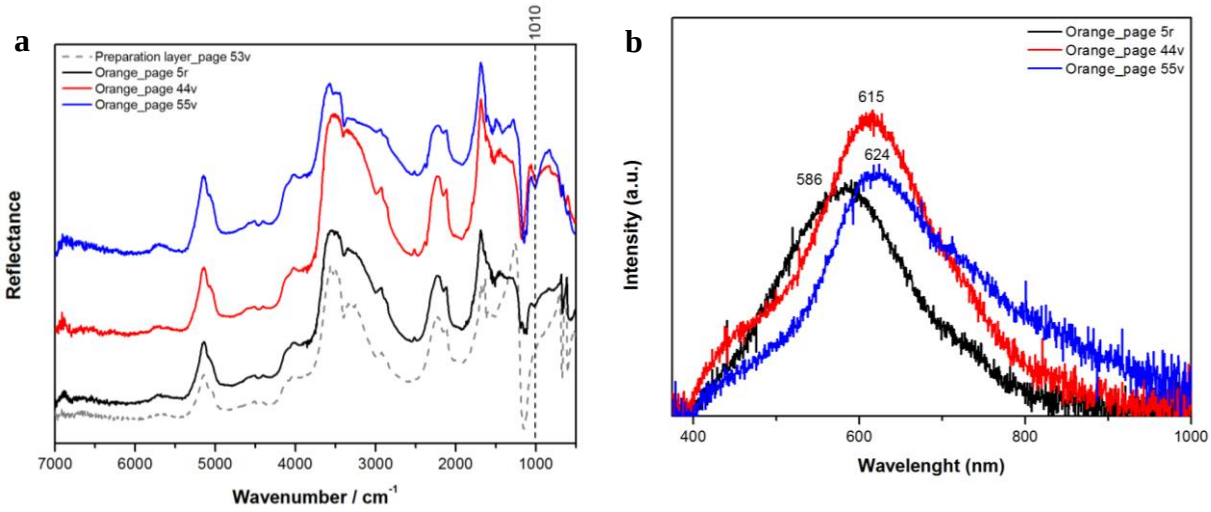

Fig. 3.12 – Spectral properties of the orange areas analysed from Codex Borgia: a) MIR in the 7000-500 cm^{-1} region; b) emission (λ_{exc}= 375 nm).

4. Conclusion

The non-invasive methods shed light into the mystical Maya Yellow. It was noticeable that for a clear distinction between flavonoids and carotenoids the reflectance and emission studies suffice, but when clay is added to obtain the hybrid pigments, Raman techniques (conventional and SERS) will perform better. It was also found that it might be possible a metal chelation, between the rings A or B of the molecules and the cations present in the clay. Also, the effect of temperature was noticeable in this study, probably because it promotes the creation of oxidized species, mentioned by Doménech-Carbó A. *et al*. [29] and it was also found that the original dye is accompanied by several deprotonated species depending on the pH. It is important to state that, if any of these dyes could be considered to be present in Mayan codices, then the recipe of preparation could not be the one described by Reyes-Valerio for Maya blue.

Several hypotheses appear: the Mayans had different preparation methods for the Mayan hybrids; the Maya yellow hybrids prepared did not contain flavonoids as their main chromophore, but carotenoids, which are less susceptible to change with increasing pH. However, a more important hypothesis is pondered: the Mayans did not use palygorskite as a support for the yellow dye, but other clays such as kaolinite. In fact, as it is possible to see in table 3.3, the pH of kaolinite is in accordance to that of the dyes, preventing them from deprotonating and changing their color. Also, it was never certain that palygorskite was the clay found in the yellow areas of the studied codices. Buti D. [3] stated that it is known that the Mesoamericans civilizations used other types of clay available to them, and in fact in Codex Tro-Cortesianus kaolinite was found in the red areas. In Codex Zouche-Nuttall the yellow areas were characterized by a yellow dye supported in an unidentified clay (see Annex 5). Doménech-Carbó A. *et al*. [29] also found that a higher amount of flavonoid is found in specimens prepared with kaolinite than with palygorskite.

It might be easy to assume that the Maya chemistry was equal for all the colors, and that the same type of recipe followed each dye. However, this might be more complex than it seems, being that the Mesoamericans might have found that different dyes could work better to their desires if matched with different clays.

The UV-Vis and portable conventional Raman do not need sampling, and therefore are non-invasive to the works of art, the codices. The SERS is still invasive, although a method is being developed that will allow the measurements without the need to remove a sample [20]. It was found that, although the electronic spectroscopy can give information about the color, which was found useful in the Maya yellow replica study, the vibrational technique can give more information about how the dye connects with the clay, and for this becomes very useful, as seen in the simplified Maya replica study. Further investigation is needed, in regards to the pH effect in several of the molecules, has well as identification of the bands in SERS.

The information obtained in this project will be further applied for the interpretation of data acquired in-situ previously and recently on the Borgia and the Vatican codices.

5. References

[1] Haude M.E., 1998, *Identification of colorants on maps from the early colonial period of new Spain* (Mexico), Journal of the American Institute for Conservation, Vol. 37, No. 3 (1), pp. 240-270

[2] Wallert A., 1994, *On some natural organic yellow colorants in Aztec codices: the Florentine codex,* Mexico, Cancun, Materials Research Society, Symposium of Materials Issues in Art and Archaeology, Vol IV, pp. 653-662

[3] Buti D., 2012, *Multi-technique approach for the in situ study of ancient manuscripts*, PhD thesis in "Scienza per la Conservazione dei Beni Culturali", Settore Scientifico Disciplinare CHIM/02-CHIM/12

[4] Domenici D., Buti D., Miliani C., Brunetti B. and Sgamellotti A., 2014, *Non-invasive analyses of pre-hispanic Mesoamerican codices*, Science and Art, The Painted Surface, Royal Society of chemistry, Editors Sgamellotti A., Brunetti B. and Miliani C., Chapter X

[5] Miliani C., Rosi F., Brunetti B. and Sgamellotti A., 2010, *In situ noninvasive study of artworks: the MOLAB multitechnique approach*, American Chemical Society, Accounts of chemical research, Vol. 43, Nº 6, pp. 728-738

[6] Miliani C., Domenici D., Clementi C., Presciutti F., Rosi F., Buti D., Romani A., Laurencich Minelli L. and Sgamellotti A., 2011, *Colouring materials of pre-Columbian codices: non-invasive in situ spectroscopic analysis of the Codex Cospi*, Elsevier, Journal of Archaeological Science, doi:10.1016/j.jas.2011.10.031

[7] Buti D., Domenici D., Miliani C., García Saíz C., Gómez Espinoza T., Jímenez Villalba F., Verde Casanova A., Sabía de la Mata A., Romani A., Presciutti F., Doherty B., Brunetti B., and Sgamellotti A., 2014, *Non-invasive investigation of a pre-Hispanic Maya screenfold book: the Madrid Codex*, Elsevier, Journal of Archaeological Science, Nº 42, pp. 166-178

[8] Zetina S., Ruvalcaba J.L., Falcón T., Alatorre J.A., Yanagisawa S., Longoria M. and Hernández E., 2014, *Material study of the codex Colombino*, Royal Society of chemistry, Science and Art, The Painted Surface, Editors Sgamellotti A., Brunetti B. and Miliani C., Chapter 5.

[9] Murray H.H., 2000, *Traditional and new applications for kaolin, smectite, and palygorskite: a general overview*, Elsevier, Applied Clay Science, No 17, pp.207-221

[10] Liu P. & Zhang L., 2007, *Adsorption of dyes from aqueous solutions or suspensions with clay nano-adsorbents*, Elsevier, Separation and Purification Technology, No. 58, pp. 32-39

[11] Giustetto R., Seenivasan K., Pellerej D., Ricchiardi G., Bordiga S., 2012, *Spectroscopic characterization and photo/thermal resistance of a hybrid palygorskite/methyl red Mayan pigment*, Microporous and Mesoporous Materials, No 155, pp. 167-176

[12] Vágvölgyi V, Daniel, LM, Pinto C, Kristóf J, Frost RL, Erzsebet H, 2008, *Dynamic and Controlled Rate Thermal analysis of Palygorskite*. Journal of Thermal Analysis and Calorimetry, No 92(2), pp. 589-594

[13] Arnold D.E., Bohor B.F., Neff H., Feinman G.M., Williams P.R., Dussubieux L. and Bishop R., 2012, *The first direct evidence of pre-columbian sources of palygorskite for Maya Blue*, Elsevier, Journal of Archaeological Science, No 39, pp. 2252-2260

[14] Giustetto R. & Wahyudi O., 2011, *Sorption of red dyes on palygorskite: Shynthesis and stability of red/purple Mayan nanocomposites*, Elsevier, Microporous and Mesoporous Materials, No 142, pp. 221-235

[15] Chiari G., Giustetto R., Druzik J., Doehne E. and Ricchiardi G., 2008, *Pre-columbian nanotechnology:reconciling the mysteries of the maya blue*, J. Paul Getty Trust, Applied Physics A, Materials Science & Processing, No 90, pp. 3-7

[16] Doménech A., Doménech-Carbó M.T., Sánchez del Río M., Agredos Pascual M.L. and Lima E., 2009, *Maya Blue as a nanostructured polyfunctional hybrid organic-inorganic material: the need to change paradigms*, The Royal Society of Chemistry and the Centre National de la Recherche Scientifique, New Journal of Chemistry, No 33, pp. 2371-2379

[17] Rondão R., Seixas de Melo J.S, Bonifácio V.D. and Melo M.J., 2010, *Dehydroindigo, the forgotten indigo and its contribution to the color of Maya blue*, Journal of Physical Chemistry, Nº 114, pp. 1699-1708

[18] Vandenabeele P., Bodé S., Alonso A. and Moens L., 2005, *Raman spectroscopic analysis of the Maya wall paintings in Ek'Balam, Mexico*, Elsevier, Spectrochimica Acta Part A 61, pp 2349–2356

[19] Doménech A., Doménech-Carbó M.T., Agredos-Pascual M.L.V., 2011, *Form Maya Blue to "Maya Yellow": A connection between ancient nanostructured materials from the voltammetry of microparticles*; Angewandte Chemie int. Ed., N0 50, pp. 5741-5744
[20] Doherty B., Brunetti B., Sgamellotti A. and Miliani C., 2011, *A detachable SERS active cellulose film: a minimally invasive approach to the study of painting lakes*, Journal of Raman Spectroscopy, doi: 10.1002/jrs.2942
[21] Liu W. & Guo R., 2005, *The interaction between morin and CTAB aggregates*, Elsevier, Journal of Colloid and Interface Science, Vol 290, Nº 2, pp. 564-573
[22] Suárez M. & García-Romero E., 2006, *FTIR spectroscopic study of palygorskite: Influence of the composition of the octahedral sheet*, Elsevier, Applied Clay Science, Nº 31, pp. 154-163
[23] Kohno Y., Inagawa M., Ikoma S., Shibata M., Matsushima R., Fukuhara C., Tomita Y., Maeda Y. and Kobayashi K., 2011, *Stabilization of a hydrophobic natural dye by intercalation into organo-montmorillonite*, Elsevier, Applied Clay Science, Nº 54, pp. 202-205
[24] Oliveira L., Dantas S., Velozo E., Santos P. and Ribeiro M., 1997, *Resonance Raman investigation and semi-empirical calculation of the natural carotenoid bixin*, Elsevier, Journal of Molecular Structure, Nº 435, pp. 101-107
[25] Andersen Ø.M. & Jordheim M., 2010, *Chemistry of Flavonoid-Based Colors in Plants*, Elsevier, 3.16, pp. 547-604
[26] Wang F., Huang W., Miao X. and Tang B., 2012, *Characterization and analytical application of morin – bovine serum albumin system by spectroscopic approaches*, Elsevier, Spectrochimica Acta Part A: Molecular and Biomolecular Spectroscopy, Nº 99, pp. 373-378
[27] Delgado-Vargas F., Jiménez A.R. and Paredes-López O., 2000, *Natural Pigments: Carotenoids, Anthocyanins, and Betalains — Characteristics, Biosynthesis, Processing, and Stability*, Critical Reviews in Food Science and Nutrition, 40, nº 3, pp. 173–289
[28] Lobato K., Paese K., Forgearini J., Guterres S., Jablonski A. and Rios A., 2013, *Characterization and stability evaluation of bixin nanocapsules*, Elsevier, Food Chemistry, Nº 141, pp. 3906-3912.
[29] Doménech-Carbó A., Doménech-Carbó M.T., Osete-Cortina L., Valle-Algarraa F.M., Miliani C. and Buti D., 2014, *Isomerization and redox tuning in 'Maya Yellow' hybrids from flavonoid dyes plus palygorskite and kaolinite clays*, Elsevier, Microporous and Mesoporous Materials, Nº 194, pp.135–145
[30] Symonowicz M. & Kolanek M., 2012, *Flavonoids and their properties to form chelate complexes*, Biotechnology and Food Sciences, Nº 76 (1), pp. 35-41
[31] Rygula A., Wrobel T.P., Szklarzewicz J. and Baranska M., 2013, *Raman and UV–vis spectroscopy studies on luteolin–Al(III) complexes*, Elsevier, vibrational spectroscopy, Nº 64, pp. 21-26
[32] Ramešová Š., Sokolová R., Degano I., Bulíčková J., Žabka J. & Gál M., 2012, *On the stability of the bioactive flavonpids quercetin and luteolin under oxygen-free conditions*, Springer, Analytical and Bioanalytical Chemistry Journal, Nº 402, pp. 975-982
[33] Casanova-González E., García-Bucio A., Ruvalcaba-Sil J.L., Santos-Vasquez V., Esquivel B., Falcón T., Arroyo E., Zetina S., Roldán M.L. and Domingo C., 2012, *Surface-enhanced Raman spectroscopy spectra of mexican dyestuffs*, Journal of Raman Spectroscopy, Nº 43, pp. 1551-1559
[34] Teslova T., Corredor C., Livingstone R., Spataru T., Birke R.L., Lombardi J.R., Cañamares M.V. and Leona M., 2007, *Raman and surface-enhanced Raman spectra of flavone and several hydroxy derivatives*, Journal of Raman Spectroscopy, Nº 38, pp. 802-818
[35] Tungjai M., Poompimon W., Loetchutinat C., Kothan S., Dechsupa N. and Mankhetkorn S., 2008, *Spectrophotometric Characterization of Behavior and the Predominant Species of Flavonoids in Physiological Buffer: Determination of Solubility, Lipophilicity and Anticancer Efficacy*, The Open Drug Delivery Journal, Nº 2, pp.10-19
[36] Jurasekova Z., Domingo C., Garcia-Ramos J. V. and Sanchez-Cortes S., 2014, *Effect of pH on the chemical modification of quercetin and structurally related flavonoids characterized by optical (UV-visible and Raman) spectroscopy*, Royal Society of Chemistry, DOI: 10.1039/c4cp00864b
[37] Sánchez del Río M., Martinetto P., Reyes-Valerio C., Dooryhée E. and Suárez M., 2006, *Synthesis and acid resistance of Maya blue pigment*, Archaeometry, Vol. 48, pp. 115-130
[38] Septhum C., Rattanaphani V. and Rattanaphani S., 2006, *UV-via spectroscopic study of natural dyes with alum as a mordant*, Suranaree J. Sci. Technol. 14(1), pp. 91-97

[39] Favaro G., Clementi C., Romani A. and Vickackaite V., 2007, *Acidichromism and ionochromism of luteolin and apigenin, the main components of the naturally occurring yellow weld: a spectrophotometric and fluorimetric study*, Journal of Fluorescence, Nº 17, pp. 707-714
[40] Marković J., Marković Z., Krstić J., Milenković D., Lučić B. and Amić D., 2013, *Interpretation of the IR and Raman spectra of morin by density functional theory and comparative analysis*, Elsevier, Vibrational Spectroscopy, Nº 64, pp. 1-9
[41] Scotter M., 2009, *The chemistry and analysis of annatto food colouring: a review*, Food Additives & Contaminants, Part A, pp. 1-23
[42] Scotter M., Castle L. and Appleton G., 2001, *Kinetic and yields for the formation of coloured and aromatic thermal degradation products of annatto in foods*, Elsevier Science, Food Chemistry, N°74, pp. 365-375
[43] Scotter M., 1995, *Characterization of the coloured thermal degradation products of bixin from annatto and a revised mechanism for their formation*, Elsevier Science, Food Chemistry, N°53, pp. 177-185
[44] Pedrós R., Moya I., Goulas Y. and Jacquemont S., 2008, *Chlorophyll fluorescence emission spectrum inside a leaf*, Photochemical & Photobiological Sciences, Vol. 7, pp. 498-502
[45] Yusá-Marco D., Doménech-Carbó T., Vaccarella I., Batista dos Santos A., Vicente-Palomino S. and Fuster-López L., 2008, *Characterization of colouring compounds in annatto (Bixa orelana l.) used in historic textiles by means of UV-Vis spectrophotometry and FT-IR spectroscopy*, Arché, publicación del Instituto Universitario de Restauración del Patrimonio de la UPV, Nº 3, pp. 153-158
[46] Zich D., Zacher T., Darmo J., Szöcs V., Lorenc D. and Janek M., 2013, *Far-infrared investigation of kaolinite and halloysite intercalates using terahertz time-domain spectroscopy*, Elsevier, Vibrational Spectroscopy, Nº 69, pp. 1-7
[47] Lee P.C. & Meisel D., 1982, *Adsorption and surface-enhanced Raman of dyes on silver and gold sols*, Journal of Physical Chemistry, vol. 86, No 17, pp. 3391-3395

Annex 1 – Materials and Methods

1.1. Laboratory analytical methods

For the **simplified Maya yellow replica**, using only the dying agent, morin or bixin, the dyes were produced adapting the recipe proposed by Reyes-Valerio [37]. As stated by Buti D. (2012), the ratio for the preparation of Maya blue is 1% in weight of organic component. However, tests performed with annatto by Buti D. [3], showed that 1% is not sufficient for yellow dyes, since indigo has a higher tinting strength. Therefore, the ratio for the preparation of yellow dyes was fixed at 20% of organic component. The morin supplied by Aldrich Chem Co. (Morin hydrate powder, 95%), since it was in powder needed no pre-preparation. However, the annatto seeds, supplied by Kremer Pigmente, needed a pre-preparation for the extraction of the coloring powder. The seeds were grinded for 15-20 minutes, and then, after obtaining about 100g, the raw grinded material was placed in a mixture of water and ethanol (50/50) – 500 ml of water and ethanol for 50 g of material. The mixture was left to stir during two days. After this time, the grains were washed with water in order to remove more dye. The remaining water (about two liters) was then left to settle for three days and then placed in a centrifuge, to separate the solvent from the dye.

The dye-clay mixture (20% or w/w of dye) was prepared by finely grinding them in an agate mortar for 30 minutes (no water added). Two clays were chosen: Palygorskite (powder; 558903; Kremer Pigmente) and Kaolinite (powder; 58250; Kremer Pigmente). Five aliquots were submitted to different temperatures for one hour, namely 140, 160, 180, 200 and 220ºC. These temperatures were chosen because it has been proved that the loss of both zeolitic and hygroscopic water occurs until 200°C in palygorskite. Also, to understand the degradation of the substance, all the raw materials, dyes and clays, were submitted to the same range of temperatures. An unheated sample of each mixture was also kept to better understand the roll of the temperature.

After the heating all the samples, these were washed with distilled water in constant stirring for 20 minutes, to remove any color responsible molecule that was not attached to the clay. In order to separate the two phases, it was used a centrifuge. Effectively, the complex clay + dye remained in the bottom. To remove the rest of the water molecules, after separating the phases and removing the excess water, the samples were all placed in a hoven at 50°C for one day.

Because the color of the annatto samples was not satisfactory, it was proposed that a higher percentage of colorant would be necessary. Therefore, it was prepared samples of 50% of annatto, following the same procedure of preparation, heating and washing as for the other samples. Because it is clear that at 180ºC the molecule starts to suffer degradation, the 50% annatto samples were only heated at 140º and 160ºC.

For the study of the **Maya yellow replica**, the samples prepared in 2012 by Buti D. (20% dyestuff), were analyzed through UV-vis emission and reflectance, conventional Raman and SERS (for those species that presented great fluorescence in the conventional Raman method). The author prepared the dyestuff following the recipe proposed by Reyes-Valerio [37]. Four species were chosen:

Fustic (wood provided by Kremer Pigmente), Orange and Yellow Cosmos (cosmos seeds; La Semeria), Orange and Yellow Marigold (fresh plant; local producers and national cultivation) and Zacatlaxcalli (fresh plant; harvested in Mexico). Because these samples were only heated at 90-100ºC at the time, a re-heating at 140ºC was necessary, followed by washing of the samples. Because the colors were not satisfactory, a new recipe was proposed adapting the recipe from Reyes-Valerio. This modified recipe had no water present in the preparation of the samples and it was later found that no washing should follow the heating. In fact, the presence of water clearly disrupted the colors, especially those made with palygorskite (see Annex 4). Also, the amount of dyestuff was raised to 50%.

Reyes-Valerio recipe:

As stated in Synthesis and acid resistance of Maya blue pigment, by Sánchez del Río M., Martinetto P., Reyes-Valerio C., Dooryhée E. and Suárez M., 2006 [37]:

"*Reyes-Valerio succeeded in making synthetic acid-resistant Maya blue using sacalum (palygorskite) and añil leaves. Several detailed formulae to prepare the pigment are described in detail in his book (Reyes-Valerio 1993). He followed these steps: (1) Fermentation or maceration. In a recipient of 0.5 l, the añil leaves (fresh or dried) are placed in a proportion of 3–5 g for each 100 ml of distilled water. Then 1,0–1,5 g of palygorskite (perhaps mixed with other clays) is added. The amount of clays must not surpass the limit of 1,5 g per 5 g of leaves in 100 ml of water. These ingredients are stirred frequently…(2) Removal of leaves, agitation and oxygenation. The leaves are removed using a mesh. The liquid is then oxygenated…by using a stirrer. The process is then stopped, and the mixture is allowed to rest for 30 min. The dyed clay particles should then be deposited at the bottom of the recipient. (3) Filtering. The mixture is filtered using a paper filter (such as a Whatman no. 1). The filtered liquid (of a yellowish colour) is discarded. (4) Drying and heating process. The filter paper with the sediment is placed in a laboratory heater. The temperature should not be higher than 90–100ºC.*"

1.2. Analytical methods

UV-vis reflectance spectroscopy

The reflectance spectra were collected using UV-vis/NIR spectrophotometer Jasco V-570 with double beam system with a single monochromator. The excitation source is a deuterium–halogen lamp and a ILN-472 integrating sphere attachment, internally coated with $BaSO_4$ and of 150 mm inside diameter, used to collect and transfer the reflectance signals either to a photomultiplier tube (UV-visible region) and to a PbS photoconductive cell (NIR region). Spectra were recorded in the range between 200 and 1600 nm, using a spectral band width of 5 nm in the UV-visible region and of 20 nm in the NIR region. Measurements were performed on solid state samples using a dedicated powder sample holder in the Jasco ILN-472. The darker colors would create saturation, so they were mixed with $BaSO_4$ (0,05g of $BaSO_4$ per 0,1 g of sample).

UV-vis emission spectroscopy

The emission spectra were collected using a portable fluorimeter. The excitation was performed at 375 nm and 445 nm, using a suitable couple of long-bandpass filters (constant transmittance in the emission spectral range). The laser power used was 5 mW for all samples. The AvaSoft software controls the acquisition of the spectra in the 200 - 1100 nm range.

In some samples there was a clear interference of chlorophyll. Therefore, some maxima cannot be measured properly. Above 160ºC the chlorophyll begins to degrade and does not distort the spectra anymore. The maxima corresponding to the chlorophyll were removed for clarity.

IR spectroscopy

Transmittance FT-IR spectra of the samples were recorded using a JASCO FTIR 470-plus spectrophotometer. The instrumentation is made up of a Genzel interferometer and a Globar source for the infrared; the detector is pyroelectric DTGS (deuterated triglycine sulphate). The spectra have been collected in a KBr pellet in the range 4000-375 cm^{-1} with a spectral resolution of 2 cm^{-1} and acquiring 200 scans.

Conventional Raman Spectroscopy and Surface-Enhanced Raman Spectroscopy (SERS)

The Raman and SERS spectra were collected using a Jasco NRS-3100 spectrometer coupled to an optical microscope with four different Olympus magnification objectives (5x, 20x, 50x and 100x) and equipped with an Argon laser source at 514 nm and 785 nm. The laser power at the sample was 2-2,5 mW at 514 nm and a maximum of 18 mW at 785 nm with minimum attenuator. The instrument is equipped with a 1200 lines/mm grating providing a resolution of approximately 1 cm^{-1} and a CCD detector Peltier cooled to -50° C. Spectra were acquired with 5 sec and 10 accumulations.

SERS method: The SERS was employed with silver colloids. Citrate-reduced colloids were prepared according to the Lee and Meisel [47] procedure by reduction of silver nitrate (Aldrich) with sodium citrate (Aldrich). Then, 200 µl of colloid was added to 50 µl of magnesium sulphate. SERS analyses were carried out by adding a 5 µl drop of magnesium sulphate aggregated colloid directly onto the powdered samples.

Annex 2 – Simplified Maya yellow replica

2.1. Temperature effect

Morin

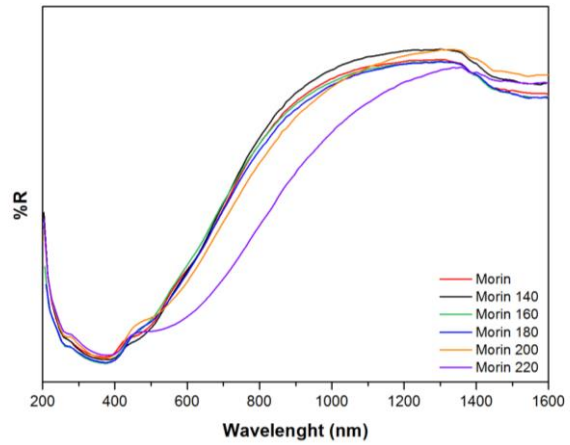

Fig. A.1 – Reflectance spectrum of morin, with and without heating.

It has been reported by Septhum C. *et al*. [38], that the morin in aqueous solution without pH control is characterized by two major absorption bands at 378 nm (B-ring cinnamoyl system) and 261 nm (absorption involving the A ring). The spectrum of morin in the solid state (Fig. A.1) is characterized by a band I at 368 nm and two shoulders at higher wavelenghts, while band II is not visible in reflection mode due to spectral distortion at low wavelenght. The hypsochromic shift of band I in the solid state with respect to solution can be ascribed to the formation of H-type aggregates, as reported for morin in high concentrated solution [21]. It is at 220°C where the three absorbance maximas are shifted to higher wavelenghts and the maxima at 508 nm (the original peak at 467 nm suffered a bathochromic shift with increased temperatures) is more intense at this temperature. Effectively, this change begins to occur at 180°C, so it is possible to assume that the molecule has undertaken some degradation.

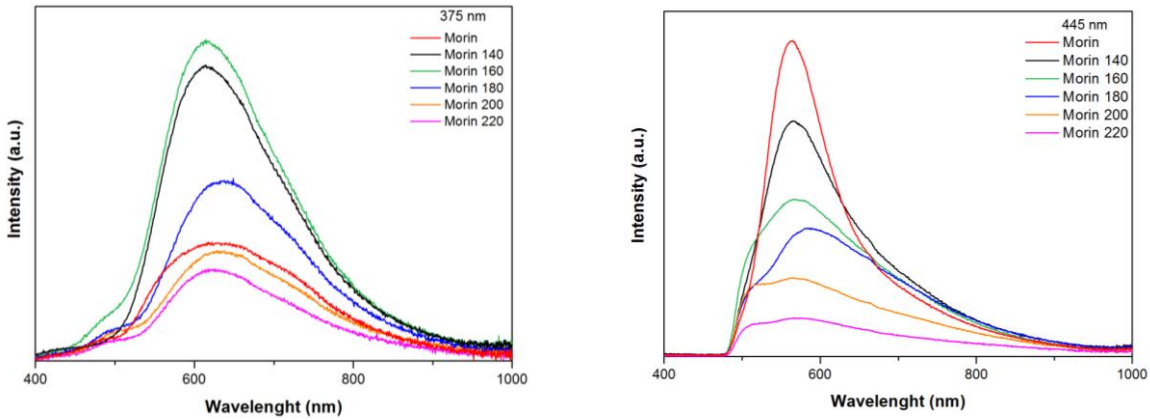

Fig. A.2 – Laser induced (λ_{exc}=375 and 445) emission spectra of morin, with heating.

The UV-Vis emission spectra of morin shows some features such as the different emission maxima with different filters. In fact there is almost a difference of 50 nm between the 375 nm filter and the 445 nm. Favaro G. *et al*. [39], made a spectrophotometric and fluorimetric study of apigenin and found that it exhibits a double emission at 430 nm (λ_{exc}=300nm) and 534 nm (λ_{exc}=357 nm). He

states that "*the origin of the double emission lies in the fact that the π,π* state of these molecules possesses a certain degree of charge transfer character due to the excited state intramolecular proton transfer from the phenolic 5-OH to the carbonyl oxygen*". In fact, morin emits a strong fluorescence with a peak at 416 nm and at 496 nm, which is due to the transition of excited-state proton transfer tautomer [26].

It is possible to state that almost no significant changes occur at the emission maxima when temperature is risen. However, the bands were not normalized, because their shape could give us more information. In fact, with the same laser intensity (5 mV, λ_{exc}= 375), the bands begin to lose signal with increasingly higher temperatures.

In the FT-IR spectrum of morin (Fig. A.3 and A.4), two important peaks are identified in the OH region, a shoulder at 3375 cm^{-1} and a band at 3248 cm^{-1}. The first one corresponds to the OH stretching of the C ring at the third carbon (C3-OH), and the second one corresponds to the OH stretching at the A ring (C2'-OH) [39]. In the lower wavenumber region it is possible to identify several peaks characteristic of morin, although it is very complex. At 1659 and 1626 cm^{-1} it is the CC stretching of C2=C3 at ring C, but also the CO stretching in rings C and A (C3-O for the peak at 1659 cm^{-1}) [40]. The peak at 1626 cm^{-1} changes intensity in relation to other peaks with increased temperature, being that the next peak (corresponding to stretching modes in the C ring) almost disappears at 220ºC. The peak at 1257 cm^{-1} also relates to the CC stretching (C and B) and to the COH bending (ring C, C3-OH) [40]. This peak and the one at 1228 cm^{-1} merge into one peak at 160ºC, therefore, some changes, especially in the B ring, are possible with increasing temperatures [40].

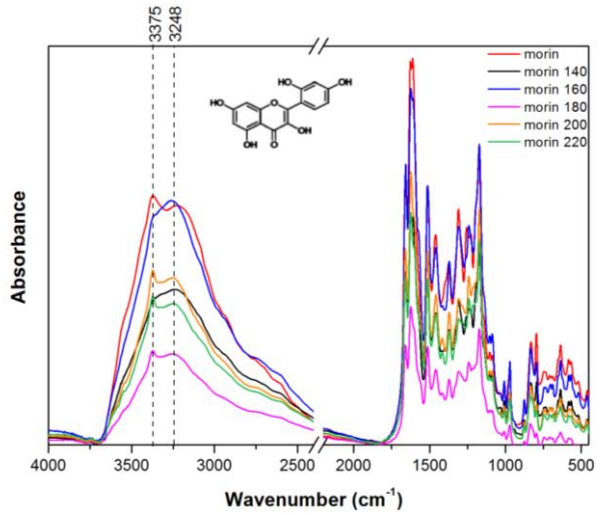

Fig. A.3 – FT-IR spectra of morin with increasing temperature (4000 – 450 cm^{-1}).

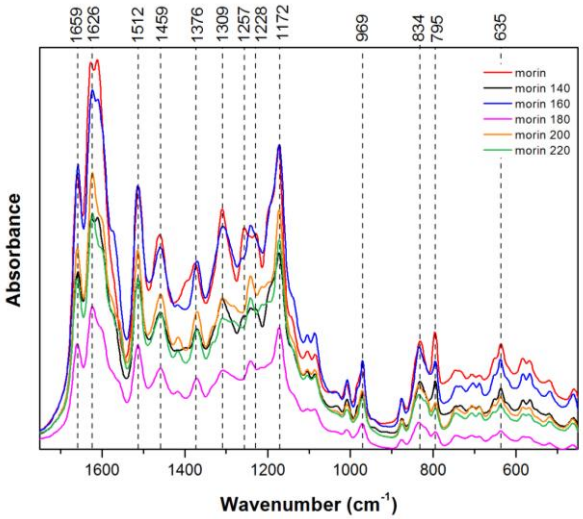

Fig. A.4 – FT-IR spectra of morin with increasing temperature (1750 – 450 cm^{-1}).

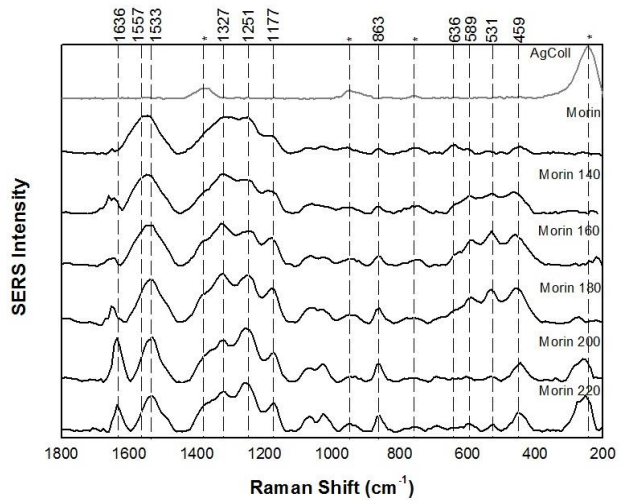

Fig. A.5 – Normalized SERS spectrum of morin, with increasing temperature (λ_{exc}=514).

There hasn't been any SERS study identifying the bands and attributing them to a determined vibrational mode. Therefore, in order to better interpret the spectrum, parallels were made with conventional Raman spectrum of morin. Although some shifts of the peaks are noticeable, it is possible to identify a few. The peak at 1636 cm^{-1} is more likely to be associated with the CC and CO stretching of ring C [40].

This peak becomes more pronounced with increased temperature. The peak 1327 cm^{-1} could be related to the COH bending and CC stretching of rings B and C. Also, the peak at 863 cm^{-1} could be attributed to HCC bending of ring B, with its correspondent peak in Raman at 876 cm^{-1}. The peak at 636 cm^{-1} is assigned to the CCO and COC bending of ring C, due to its similarity with the Raman peak at 638 cm^{-1}. This peak disappears with increasingly higher temperatures. The peaks at 589, 531 and 459 cm^{-1} are more likely related to the torsion of several CCCH bonds in the different rings [40].

Annatto

The major colouring component of annatto is the apo-carotenoid 9'-*cis*-bixin, usually refered to as *cis*-bixin. This component is soluble in most polar organic solvents to which it takes an orange colour, but because of its instability it convertes to the all-*trans* isomer which exhibits a red colour in solution [41]. The powder extracted from the annatto seeds, presents an orange colour in solution of acetone. Therefore, it could be an indication that the coloring agent present in the samples is mainly *cis*-bixin (Fig. A.6).

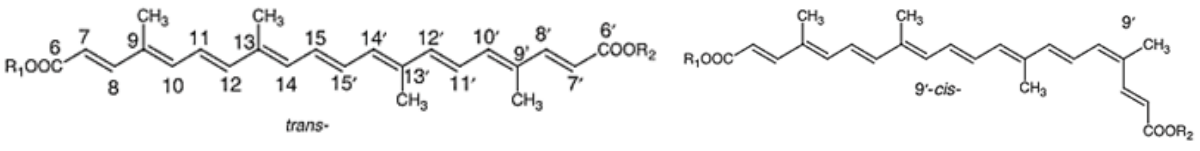

Fig. A.6 - Chemical structures of some bixin/norbixin isomers: all-*trans* isomer (left) and 9'-*cis*-bixin (right). If R_1=H, R_2=H = norbixin; if R_1=H, R_2=CH3 = bixin [41][7].

7) Scotter M., 2009, Food Additives & Contaminants, Part A, pp 1-23

The typical three close absorption bands of annatto are present (at 351, 455 and 525 nm). The very small shoulder at 351, with an hypsochromic effetc with the the increase of temperature, provides information on the type of isomer. Like predicted the very weak peak at 355 nm corresponds to the 9'*cis*-isomer [41]. In the reflectance spectrum of annatto, it is possible to see a preferable hypsochromic effect with increasingly higher temperatures.

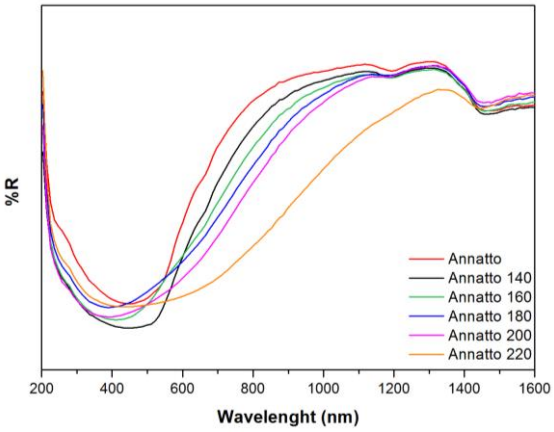

Fig. A.7 – Reflectance spectrum of annatto, with heating.

From 140ºC we can see that the peak at 351 nm has shifted ~20 nm to lower wavelengths, and the peak at 455 nm is, at 200ºC, at 391 nm. The same hypsochromic effect can be seen in the peak at 640 nm and 1463 nm. Thermal degradation of the principal annatto colouring agent 9'-*cis*-bixin, at 140°C has been shown to be thermodynamically possible by Scotter M. *et al.* [42], resulting in the irreversible formation of C17 (with the associated production of m-xylene) (Fig. A.8).

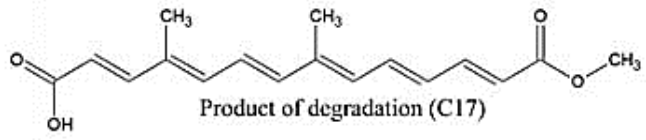

Fig. A.8 – Chemical structure of the main product of degradation from 9'-*cis*-bixin [43][8].

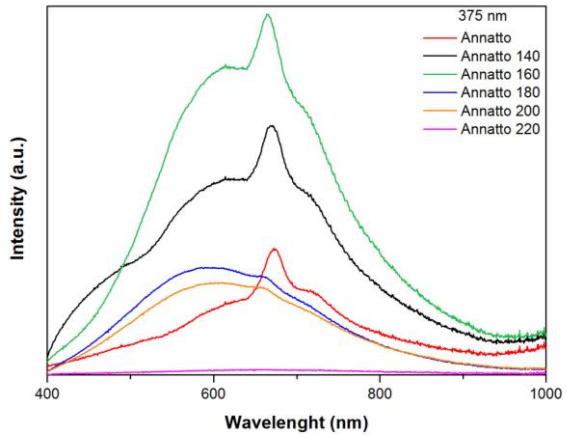

Fig. A.9 – Laser induced (λ_{exc}=375) emission spectrum of annatto, with heating.

The maxima of bixin are at higher wavelengths when compared to morin. Its analogous peak at the absorption spectrum (640 nm), provides the information necessary to identify this colorant. It is also possible to see, that a hypsochromic shift occurs with higher temperatures. There is a spectral overlap in the emission spectrum of annatto. The sharp peak at ~665 nm (λ_{exc}=375 and 445 nm) is representative of chlorophyll.

The chlorophyll-*a* fluorescence emission spectrum is characterized by a major peak at 683 nm attributable to photosystem II [44]. Because of the peaks similarities, and because it is most common in flower, it is assumable that the chlorophyll type present is type-*a* [44]. It is known that cholorophyll is extremely susceptible to degradation by heat, being noticeable that at 180ºC, the chlorophyll characteristic peak no longer exists.

8) Scotter M., 1995, Food Chemistry, N°53, pp. 177-185

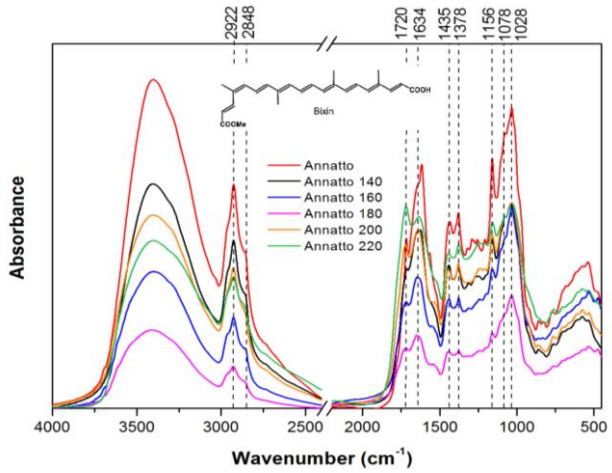

Fig. A.10 – FT-IR spectra of annatto with increasing temperature (4000 – 450 cm^{-1}).

In the FT-IR of annatto, the peaks at 2922 and 2848 cm^{-1} are very important to characterize the molecule bixin, for they correspond to the asymmetric and symmetric stretching of CH_2 groups from the hydrocarbon skeleton [45]. At 1720 cm^{-1} is the stretching of the C=O groups associated to aliphatic carboxylic acid, and at 1634 cm^{-1} is the alkenyl stretching of the C=C group.

These peaks change in intensity related to one another with increasingly higher temperatures, and it could be due to the formation of the C17. The two peaks at 1435 and 1378 cm^{-1} belong to the bending of the OH phenol (or tertiary alcohol) and to the symmetric bending of CH_3 groups, respectively [45]. The peak at 1156 cm^{-1} is also very important for the identification of bixin because it is related to the stretching of the CO group from carboxylic acid.

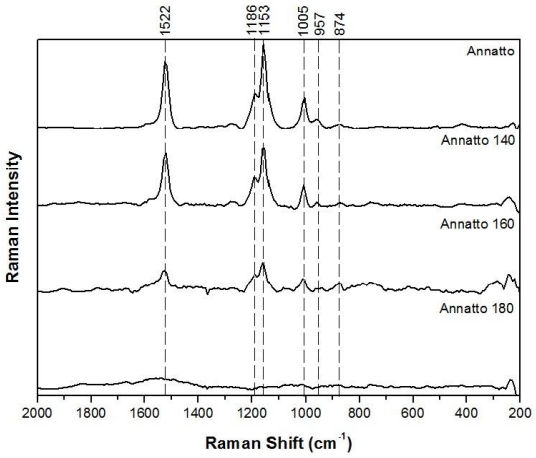

Fig. A.11 – Normalized Raman spectrum of annatto, with increaing temperature (λ_{exc}=514).

The major peaks assigned to bixin can be identified in the spectrum of Raman. The peak at 1522 cm^{-1} corresponds to the C=C stretching mode of the molecule. The peaks at 1186 and 1153 cm^{-1} are related to the CH bending and the CC stretching, respectively. Finally, the peak at 1005 cm^{-1} corresponds to the CH3 bending of bixin [24]. With the increase of temperature the spectra loses signal, therefore indicating that the molecule is degradated. In fact at 220ºC it is possible to see no similarities with the pure annatto spectrum.

Palygorskite and Kaolinite

For a better characterization of the clay-hybrid samples, it is necessary to know in extend the FT-IR bands characteristic of each clay. A thermal degradation study was also conducted, but it yield no significant results in FT-IR, i.e., the clays remain intact until 220ºC.

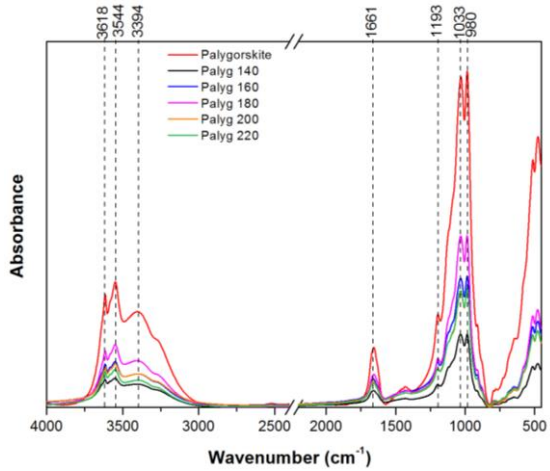

Fig. A.12 – FT-IR spectrum of palygorskite with increasing temperature (4000 – 450 cm^{-1}).

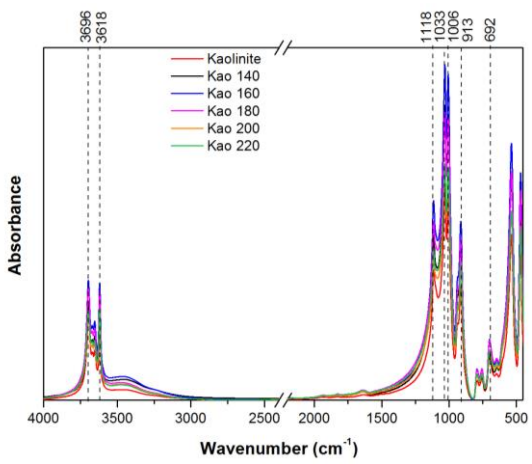

Fig. A.13 – FT-IR spectrum of kaolinite with increasing temperature (4000 – 450 cm^{-1}).

In the spectrum of palygorskite a sharp peak at 3618 cm^{-1} is extensively described in bibliography [22] and it is related to the OH stretching mode in Al_2-OH groups. Also the two bands at 3544 and 3394 cm^{-1} are assigned to water molecules (coordinated and zeolitic water) [21]. The band centered at 1661 cm^{-1} corresponds to the bending modes of absorbed and zeolitic water. The peak at 1193 cm^{-1} is characteristic of palygorskite, and as reported by Suárez M. & García-Romero E. [22], it does not appear in other clay minerals, except sepiolite. The two most intense peak in the spectrum, at 1033 and 980 cm^{-1} correspond to the stretching mode of the Si-O bond.

The OH region in kaolinite is very different from that in palygorskite. There are two very sharp peaks at 3696 and 3618 cm^{-1}, being that the first one corresponds to the OH stretching modes of inner-surface hydroxyl, reported in literature [46]. The second peak corresponds to the OH stretching of inner hydroxyl groups. At the lower wavenumber region, it is possible to identify other important peaks that correspond to the Si-O stretching modes such as the peaks at1118, 1033 and 1006 cm^{-1}. Also, another peak at 692 cm^{-1} is related to the bending mode of Si-O. Another very important peak at 913 cm^{-1} corresponds to the OH deformation of inner hydroxyl groups [46].

FT-IR is presented has an important technique for identifying between the dyes alone and also to characterize the clays. It was noticeable that the dyes began to degrade at 140ºC, and because of this, the studies of dye-clay hybrids are only presented with heating until this temperature. Also, the clays present no degradation until 220ºC.

2.2. UV-vis reflectance spectroscopy

Table A.1 *– Absorption maxima of the pure dyes and the dye-clay hybrids. The numbers inside brackets represent the maxima at 50% of dye, while the others are the maxima at 20 %.*

Morin		**λ_{max} abs (nm)**	**Annatto**		**λ_{max} abs (nm)**
Morin	without heating	258, 368, 467	**Annatto**	without heating	351, 455, 525, 640, 1463
	140°C	257, 377, 467		140°C	334, 410, 637, 1463
	160°C	261, 373, 476		160°C	322, 411, 636, 1463
	180°C	262, 379, 489		180°C	392, 1457
	200°C	270, 368, 508		200°C	391, 1457
	220°C	270, 379, 508		220°C	434, 1444
Morin@Palygorskite	Palygorskite	258, 464, 1427	**Annatto@Palygorskite**	Palygorskite	258, 464, 1427
	without heating	268, 391, 1424		without heating	414, 537, 646, 795, 1422 (260, 439, 752, 1418)
	140°C	269, 404, 507, 1422		140°C	335, 554, 808, 1422 (255, 434, 805)
	160°C	275, 404, 507, 1422		160°C	334, 554, 808, 1422
	180°C	275, 404, 505, 1425		180°C	335, 524, 808, 1422
	200°C	270, 410, 505, 1422		200°C	340, 513, 886, 1422
	220°C	270, 410, 472, 1422		220°C	340, 513, 874, 1422
Morin@Kaolinite	Kaolinite	263, 330, 1404	**Annatto@Kaolinite**	Kaolinite	263, 330, 1404
	without heating	268, 389, 480, 1404		without heating	333, 412, 552, 640, 1401 (252, 434, 658, 1403)
	140°C	270, 403, 496, 1404		140°C	301, 348, 552, 647, 858, 1401 (236, 422, 669, 1386)
	160°C	270, 390, 488, 1404		160°C	335, 661, 873, 1401
	180°C	270, 386, 495, 1404		180°C	319, 678, 887, 1401
	200°C	270, 385, 494, 1404		200°C	327, 853, 1401
	220°C	270, 389, 488, 1404		220°C	327, 872, 1401

2.3. UV-vis emission spectroscopy

Table A.2 *- Emission maxima of the pure dyes and the dye-clay hybrids. The numbers inside brackets represent the maxima at 50% of dye, while the others are the maxima at 20 % (λ_{exc}= 375 and 445 nm).*

	Morin	375 nm	445 nm		Annatto	375 nm
Morin	without heating	630	564	**Annatto**	without heating	715
	140°C	612	565		140°C	638
	160°C	614	567		160°C	614
	180°C	634	584		180°C	593
	200°C	632	566		200°C	608
	220°C	622	572		220°C	655
Morin@Palygorskite	Palygorskite	511	531/573	**Annatto@Palygorskite**	Palygorskite	511
	without heating	620	552		without heating	599 (598)
	140°C	598	585		140°C	565 (618)
	160°C	600	587		160°C	593
	180°C	600	581		180°C	550
	200°C	611	513		200°C	544
	220°C	616	513		220°C	544
Morin@Kaolinite	Kaolinite	488	515	**Annatto@Kaolinite**	Kaolinite	488
	without heating	511, 614	528		without heating	594 (679)
	140°C	512, 621	513		140°C	611 (615)
	160°C	507, 630	513		160°C	565
	180°C	507, 634	511		180°C	581
	200°C	509, 641	511		200°C	612
	220°C	504, 647	507		220°C	620

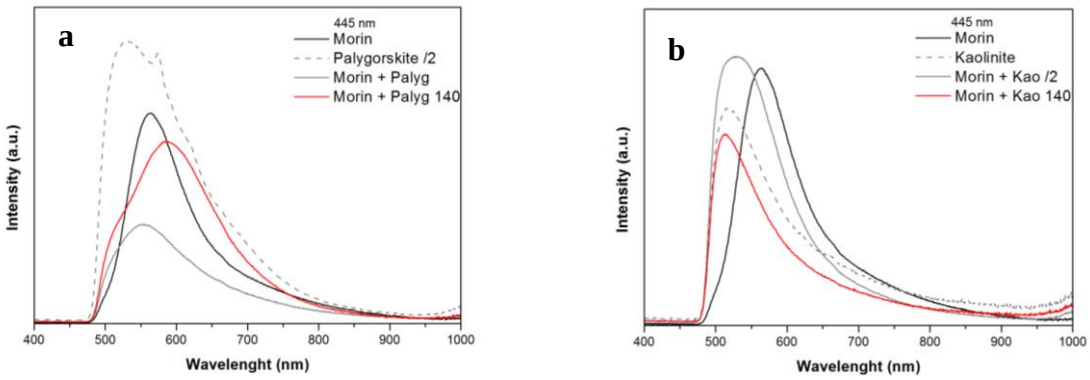

Fig. A.14 –UV-vis emission properties (λ_{exc}= 445 nm) of morin MY's unheated and heated at 140ºC. a)Morin@palygorskite and b)Morin@kaolinite.

Chlorophyll contribution to the emission spectra of Annatto:

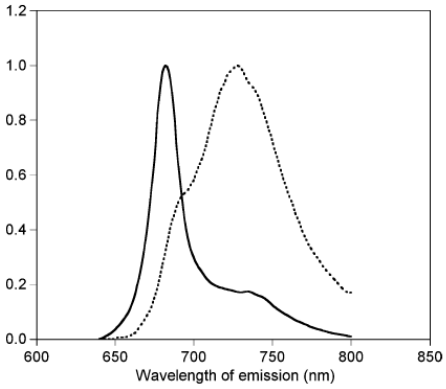

Fig. A.15 – Normalized fluorescence emission of Chlorophyll-*a*: PSII (straight line) and PSI (dotted line) [44][9].

2.4. FT-IR spectroscopy

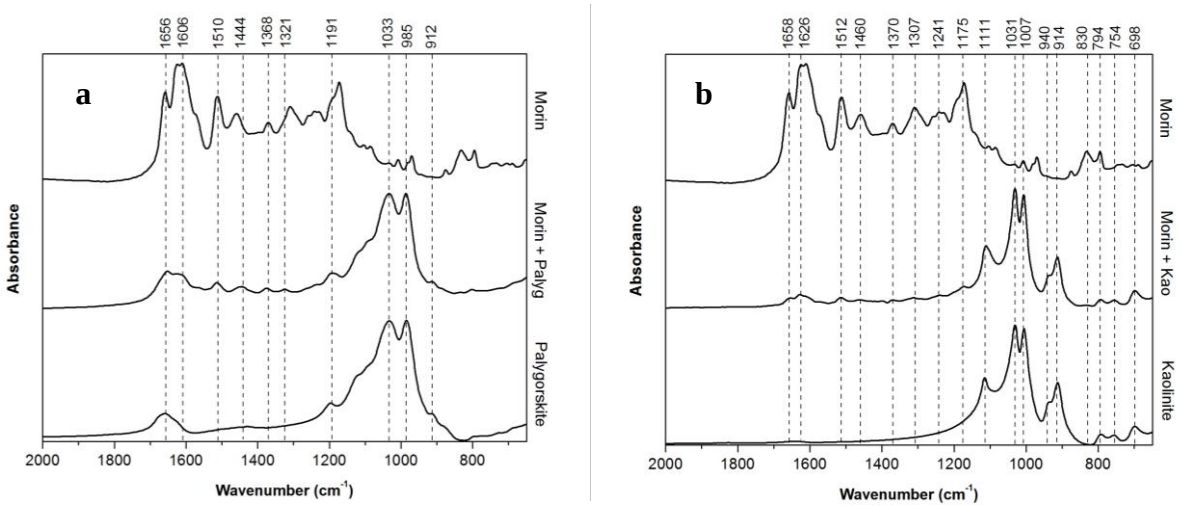

Fig. A.16 – FT-IR spectra of a) Morin@palygorskite and b) Morin@kaolinite at 140°C (2000 – 650 cm^{-1}).

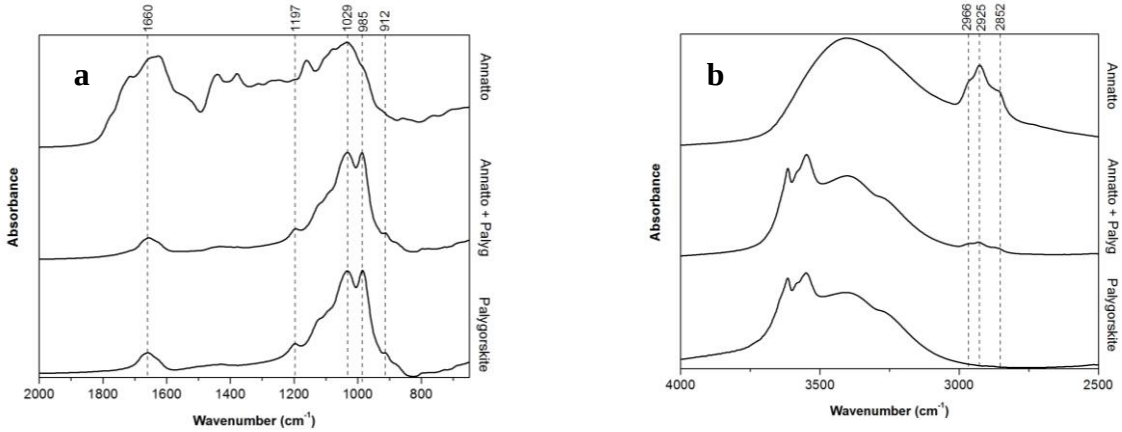

Fig. A.17 – FT-IR spectra of annatto@palygorskite at 140°C in the a) 2000 – 650 cm^{-1} region and b) 4000 – 2500 cm^{-1} region

9) Pedrós R. *et al*., 2008, Photochemical & Photobiological Sciences, Vol. 7, pp. 498-502

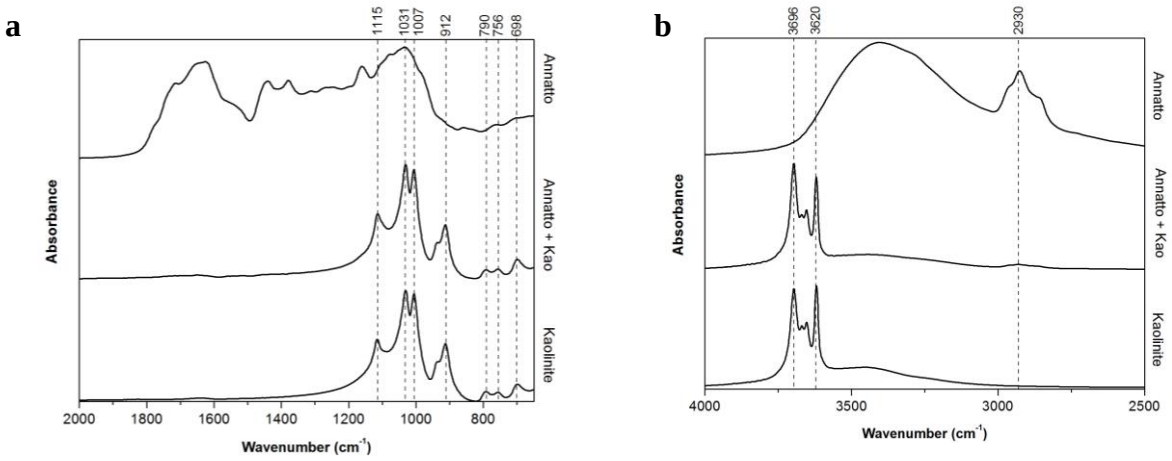

Fig. A.18 – FT-IR spectra of annatto@kaolinite at 140°C in the a) 2000 – 650 cm^{-1} region and b) 4000 – 2500 cm^{-1} region

Annex 3 - Maya yellow replica

3.1. Reyes-Valerio Method

3.1.1. UV-vis reflectance spectroscopy

Table A.3 *– Absorption maxima of the samples with the Reyes-Valerio method (λmax abs (nm)).*

Dye / Label		Reyes-Valerio Method - λmax abs (nm)	
		Heated at 100°C	Heated 140°C
Fustic	Fus	234, 333, 407, 518	262, 365, 413, 514, 1460
	Fus@Palyg	262, 344, 412, 519, 1447	262, 349, 412, 519, 1455
	Fus@Kao	263, 336, 420, 1418	262, 344, 423, 1411
Orange Cosmos	OC	215, 265, 330, 400, 523, 631, 1217, 1470	240, 330, 400, 511
	OC@Palyg	262, 332, 395, 495, 1416	259, 333, 385, 492, 1414
	OC@Kao	262, 330, 395, 491, 1399	259, 325, 388, 511, 1398
Yellow Cosmos	YC	234, 330, 395, 1460	237, 333, 400, 1466
	YC@Palyg	261, 330, 400, 1420	260, 328, 404, 1415
	YC@Kao	270, 330, 382,1400	262, 328, 421, 1384
Orange Marigold	OM	228, 263, 334, 376, 663, 1483	230, 332, 390, 669, 1488
	OM@Palyg	261, 380, 596, 1416	256, 396, 582, 1422
	OM@Kao	265, 378, 485, 677, 1400	262, 379, 664, 1400
Yellow Marigold	YM	232, 263, 332, 378, 669, 1458	220, 259, 330, 404, 667, 1477
	YM@Palyg	259, 378, 563, 1418	254, 393, 596, 1422
	YM@Kao	269, 378, 485, 673, 1400	269, 378, 492, 675, 1400
Zacatlaxcalli	Zac	228, 261, 368, 515, 1464	228, 261, 368, 515, 1466
	Zac@Palyg	257, 378, 525, 1416	265, 330, 382, 524, 1417
	Zac@Kao	265, 336, 391, 508, 1401	262, 333, 415, 508, 1400

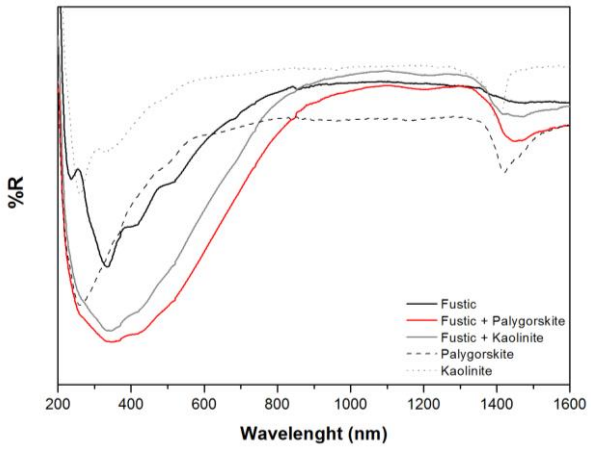

Fig. A.19 – Reflectance spectra of fustic@clay.

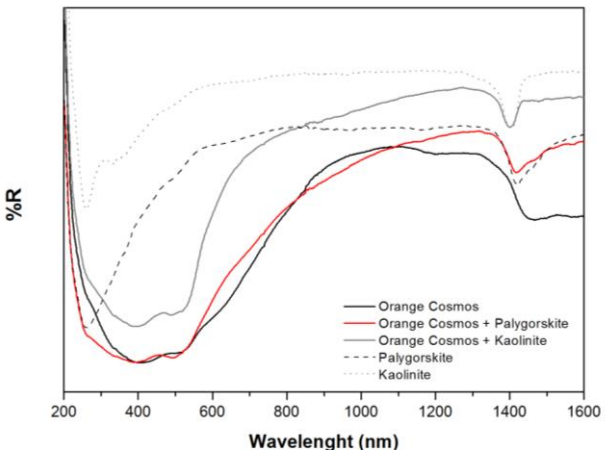

Fig. A.20 – Reflectance spectra of orange cosmos@clay.

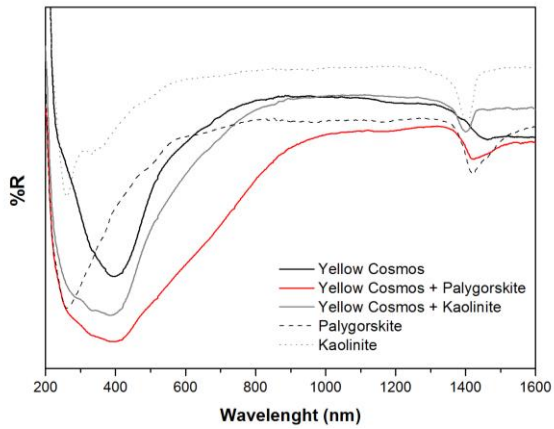

Fig. A.21 – Reflectance spectra of yellow cosmos@clay.

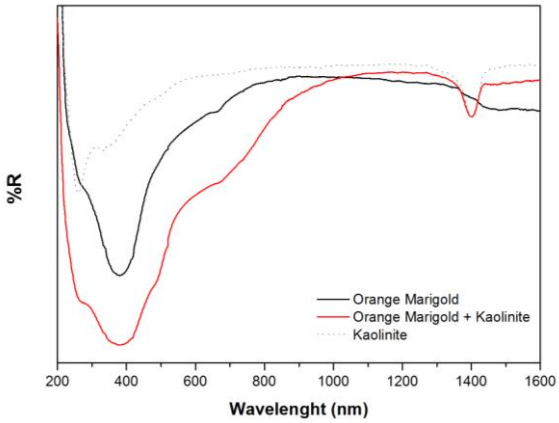

Fig. A.22 – Reflectance spectra of orange marigold@kaolinite.

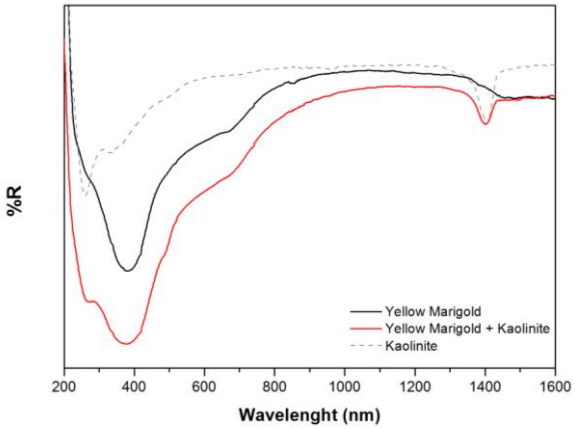

Fig. A.23 – Reflectance spectra of Yellow Marigold@kaolinite.

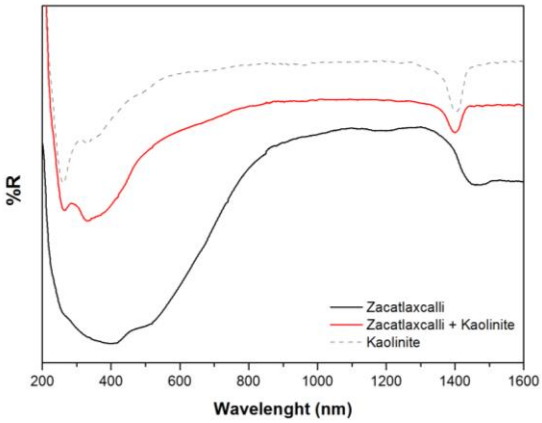

Fig. A.24 – Reflectance spectra of Zacatlaxcalli@kaolinite.

3.1.2. UV-vis emission spectroscopy

Table A.4 *- Emission maxima of the Reyes-Valerio method. With red are represented the uncertain maxima because of their closeness to the filter or to other bands (λ_{exc}= 375 nm).*

Reyes-Valerio Method		Heated at 100ºC	Heated 140ºC
Fustic	Fus	415, 610	412, 610
	Fus@Palyg	430, 535	460, 550
	Fus@Kao	430, 540	425, 520
Orange Cosmos	OC	595	600
	OC@Palyg	510, 560, 580	490, 550, 580
	OC@Kao	495, 580, 720	480, 580, 720
Yellow Cosmos	YC	600	640
	YC@Palyg	515	515
	YC@Kao	530	540
Orange Marigold	OM	585, 720	595, 710
	OM@Palyg	540	520
	OM@Kao	470, 550, 720	475, 545, 725

Yellow Marigold	**YM**	440, 560, 715	600, 715
	YM@Palyg	470, 540, 720	445, 520
	YM@Kao	480, 545, 715	475, 540, 720
Zacatlaxcalli	**Zac**	470, 635	635
	Zac@Palyg	500, 550	490
	Zac@Kao	515	520

The spectra at 445 nm were excluded because the bands were cut for their closeness to the filter and also because it did not add information to that presented at λ_{exc}=375.

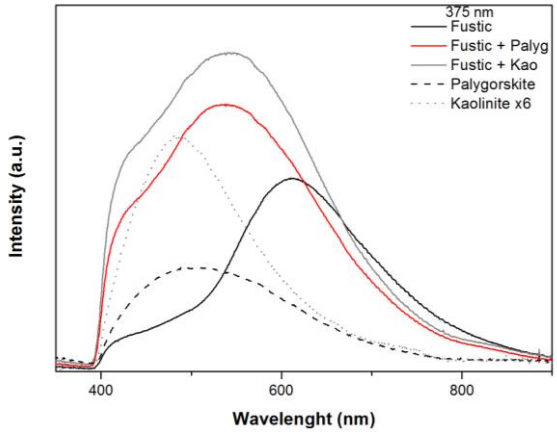

Fig. A.25 – Laser induced (λ_{exc}=375) emission spectra of fustic@clays.

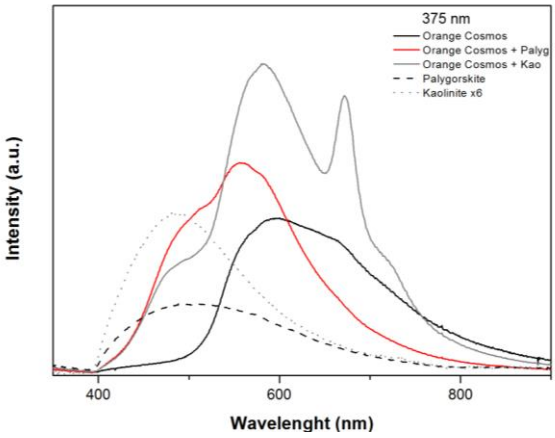

Fig. A.26 – Laser induced (λ_{exc}=375) emission spectra of orange cosmos@clays.

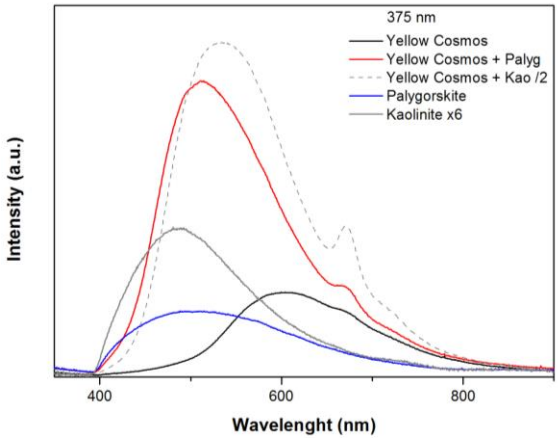

Fig. A.27 – Laser induced (λ_{exc}=375) emission spectra of yellow cosmos@clays.

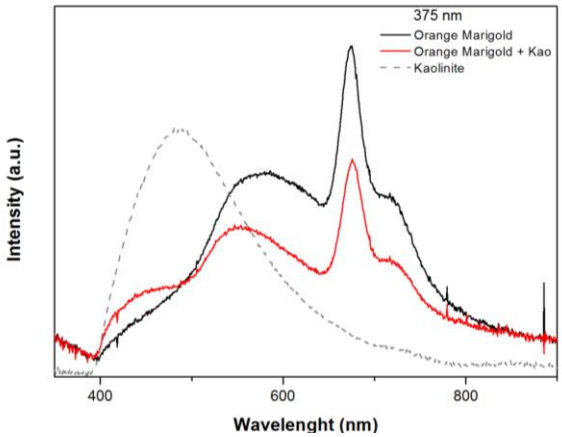

Fig. A.28 – Laser induced (λ_{exc}=375) emission spectra of orange marigold@kaolinite.

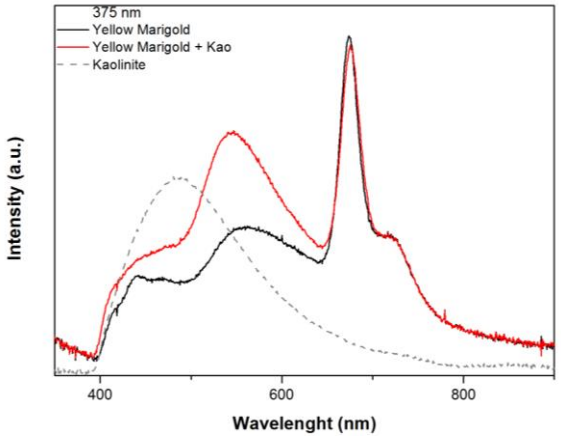

Fig. A.29 – Laser induced (λ_{exc}=375) emission spectra of yellow marigold@kaolinite.

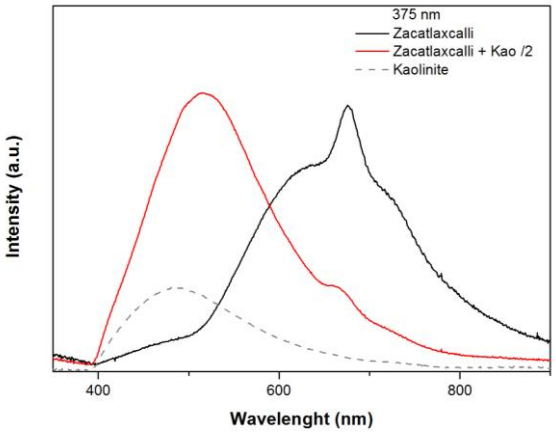

Fig. A.30 – Laser induced (λ_{exc}=375) emission spectra of zacatlaxcalli@kaolinite.

3.2. Modified Method

3.2.1. UV-vis reflectance spectroscopy

Table A.5 *– Absorption maxima of the samples with the Modified method (λmax abs (nm)).*

Dye / Label		Modified Method - λmax abs (nm)	
		Not-heated	Heated 140ºC
Fustic	Fus	234, 333, 407, 518	262, 365, 413, 514, 1460
	Fus@Palyg	256, 331, 415, 508, 1417	254, 333, 415, 510, 1422
	Fus@Kao	241, 335, 405, 518, 1400	241, 330, 410, 518, 683, 1400
Orange Cosmos	OC	215, 265, 330, 400, 523, 631, 1217, 1417	240, 330, 400, 511,
	OC@Palyg	257, 328, 400, 505, 645, 1417	260, 331, 400, 505, 645, 1428
	OC@Kao	257, 325, 400, 522, 629, 1406	257, 325, 400, 522, 626, 1400
Yellow Cosmos	YC	234, 330, 395, 1460	237, 333, 400, 1466
	YC@Palyg	220, 265, 330, 400, 650, 1425	220, 265, 330, 400, 650, 1433
	YC@Kao	213, 262, 331, 400, 667, 1400	213, 267, 300, 400, 667, 1400
Orange Marigold	OM	228, 263, 334, 376, 663, 1483	230, 332, 390, 669, 1488
	OM@Palyg	215, 265, 385, 660, 1420	215, 260, 389, 668, 1450
	OM@Kao	218, 268, 392, 667, 1400	218, 268, 392, 660, 1400
Yellow Marigold	YM	232, 263, 332, 378, 669, 1458	220, 259, 330, 404, 667, 1477
	YM@Palyg	216, 284, 392, 667, 1455	216, 300, 392, 659, 1417
	YM@Kao	211, 261, 392, 669, 1410	211, 261, 389, 665, 1400
Zacatlaxcalli	Zac	228, 261, 400, 515, 1464	228, 261, 400, 515, 1466
	Zac@Palyg	211, 264, 330, 378, 486, 1425	219, 264, 330, 378, 489, 1425
	Zac@Kao	214, 264, 330, 375, 493, 1403	214, 269, 330, 375, 482, 1403

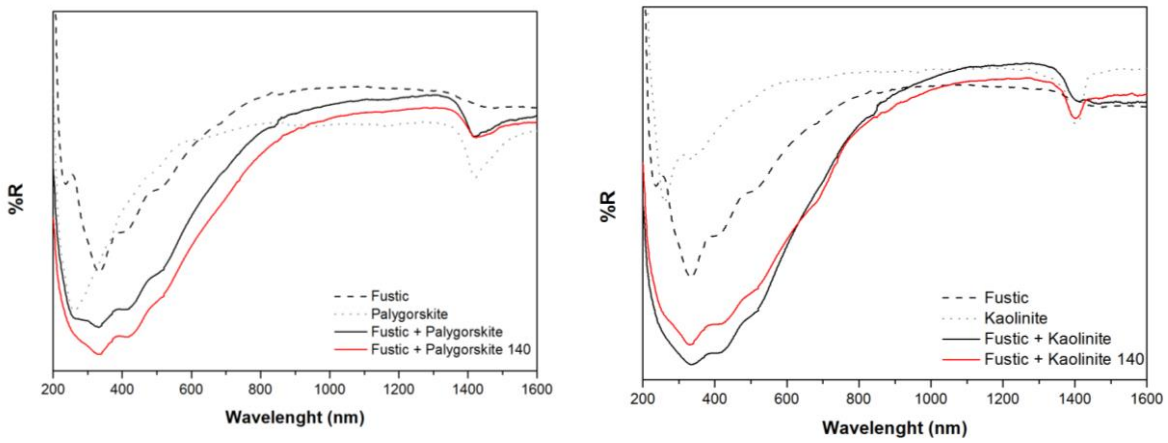

Fig. A.31 – Reflectance spectra of fustic@clay heated at 140ºC.

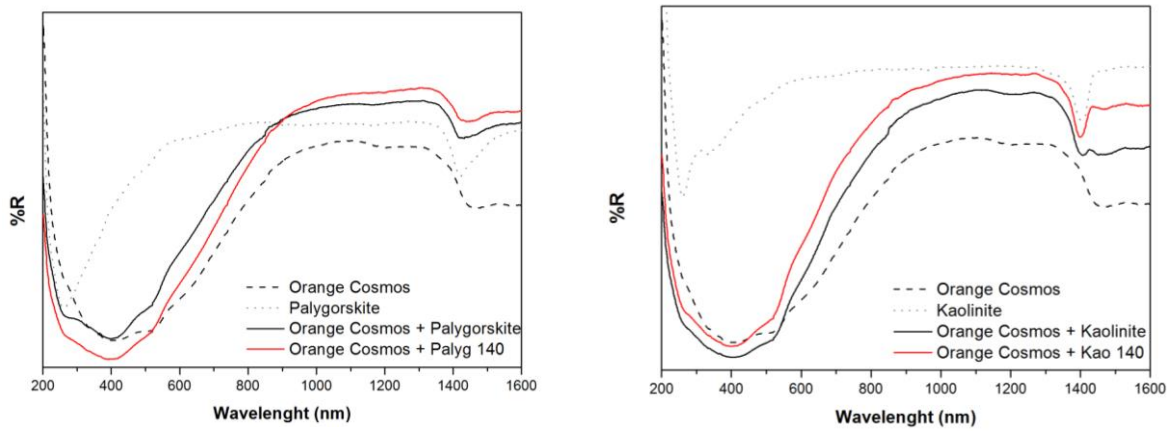

Fig. A.32 – Reflectance spectra of orange cosmos@clay heated at 140ºC.

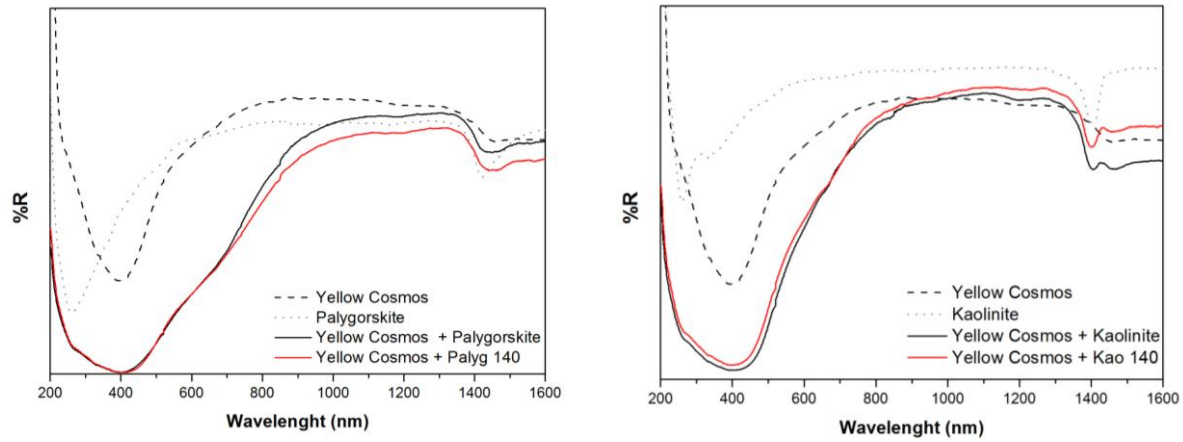

Fig. A.33 – Reflectance spectra of yellow cosmos@clay heated at 140ºC.

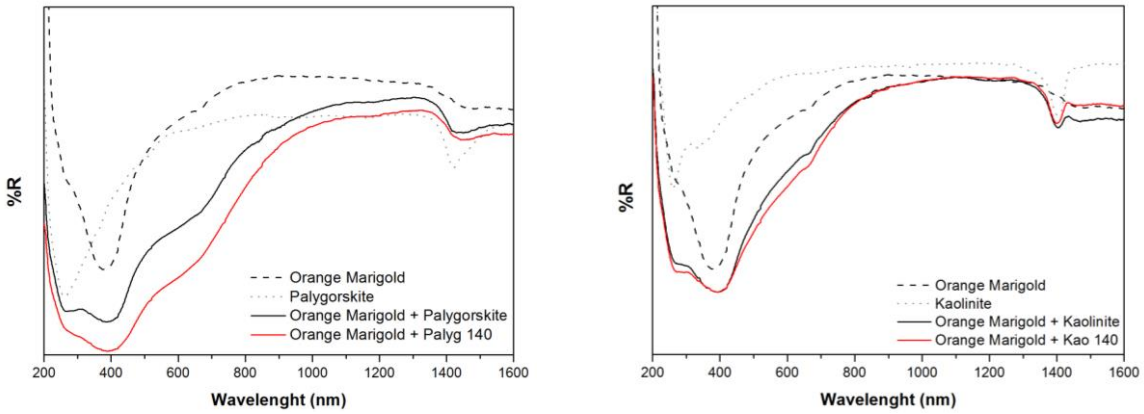

Fig. A.34 – Reflectance spectra of orange marigold@clay with heated at 140ºC.

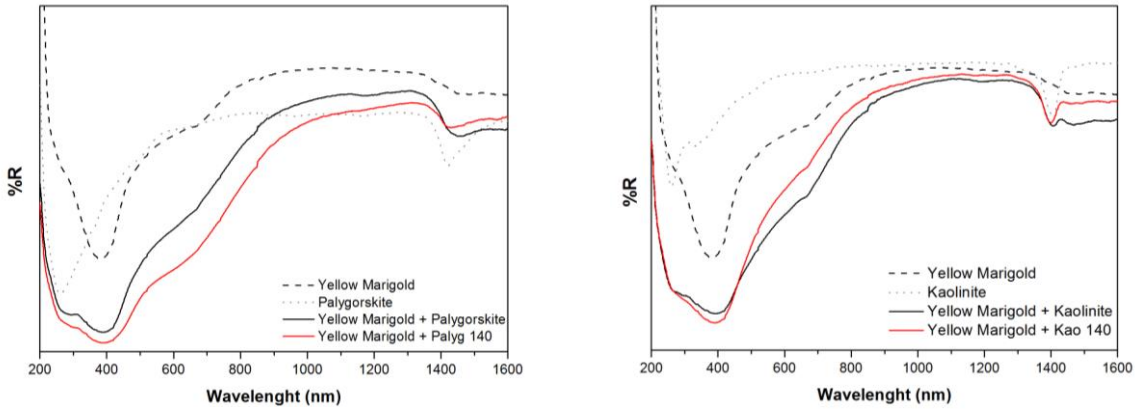

Fig. A.35 – Reflectance spectra of yellow marigold@clay heated at 140ºC.

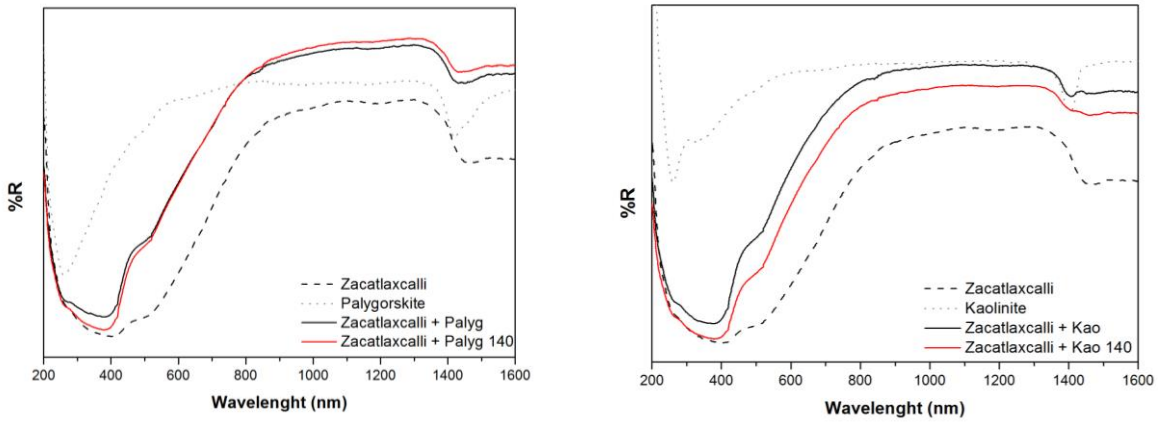

Fig. A.36 – Reflectance spectra of zacatlaxcalli@clay heated at 140ºC.

3.2.2. UV-vis emission spectroscopy

Table A.6 *- Emission maxima of the Modified method. With red are represented the uncertain maxima because of their closeness to the filter or to other bands (λ_{exc}= 375).*

Modified Method		Not-heated	Heated 140°C
Fustic	Fus	415, 610	412, 610
	Fus + Palyg	495, 595	510, 595
	Fus + Kao	415, 495, 600	415, 512, 585
Orange Cosmos	OC	595	600
	OC + Palyg	490, 610	480, 610
	OC + Kao	610	610
Yellow Cosmos	YC	600	640
	YC + Palyg	605	605
	YC + Kao	600	600
Orange Marigold	OM	585, 675, 720	595, 675, 710
	OM + Palyg	475, 540, 715	445, 545, 725
	OM + Kao	475, 545, 720	475, 545, 720
Yellow Marigold	YM	440, 560, 715	600, 715
	YM + Palyg	475, 540, 715	485, 535
	YM + Kao	475, 550, 715	560, 720
Zacatlaxcalli	Zac	470, 635	635
	Zac + Palyg	490, 615	490, 610
	Zac + Kao	450, 607	450, 610

When the spectra had to be augmented or divided for a better visualization an indication of the multiplication/division is indicated next to the name (e.g. Orange Marigold + Palyg 140 x2 or /2).

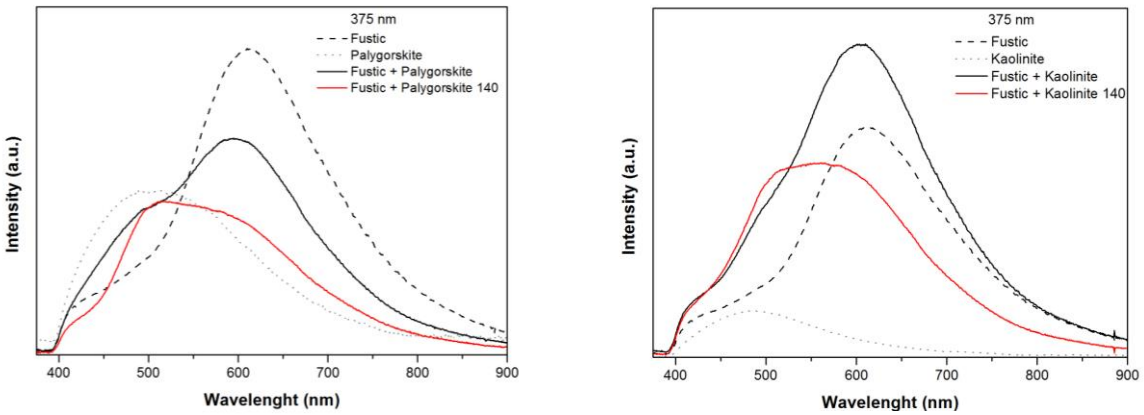

Fig. A.37 – Laser induced (λ_{exc}=375) emission spectra of fustic@clays heated at 140°C.

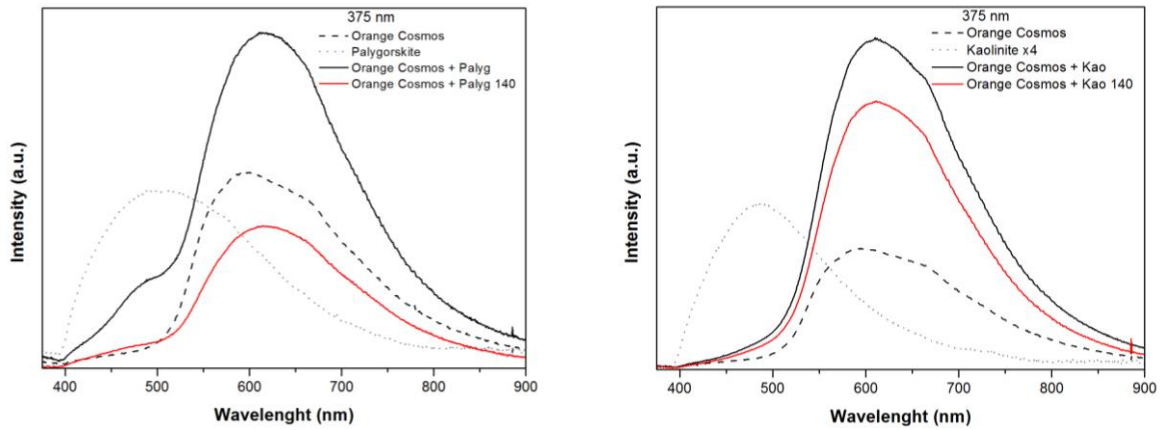

Fig. A.38 – Laser induced (λ_{exc}=375) emission spectra of orange cosmos@clays heated at 140ºC.

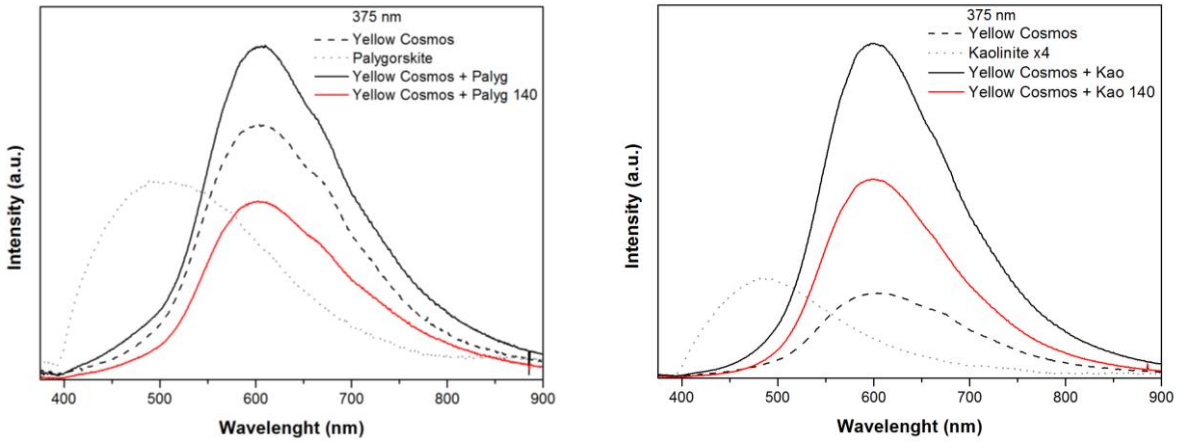

Fig. A.39 – Laser induced (λ_{exc}=375) emission spectra of yellow cosmos@clays heated at 140ºC.

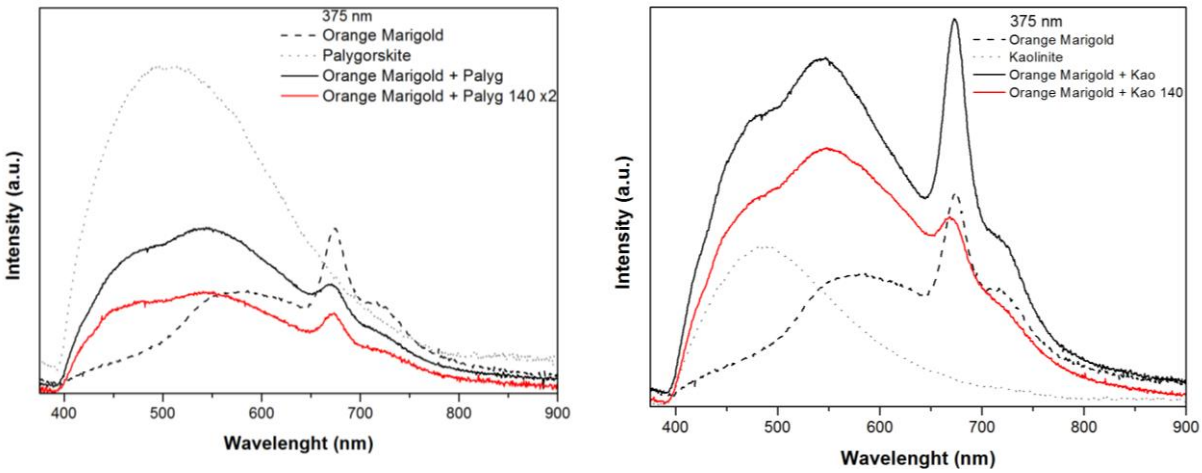

Fig. A.40 – Laser induced (λ_{exc}=375) emission spectra of orange marigold@clays heated at 140ºC.

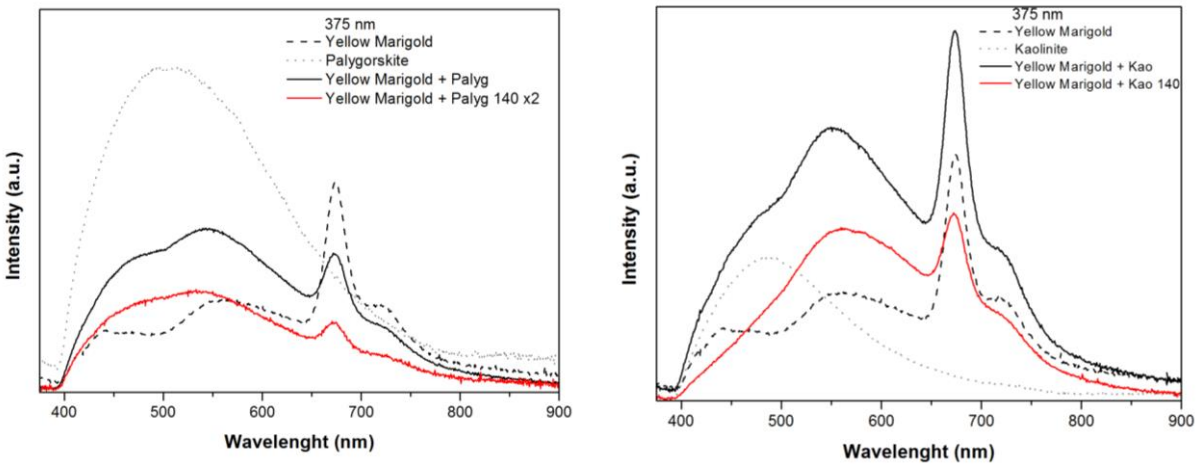

Fig. A.41 – Laser induced (λ_{exc}=375) emission spectra of yellow marigold@clays heated at 140ºC.

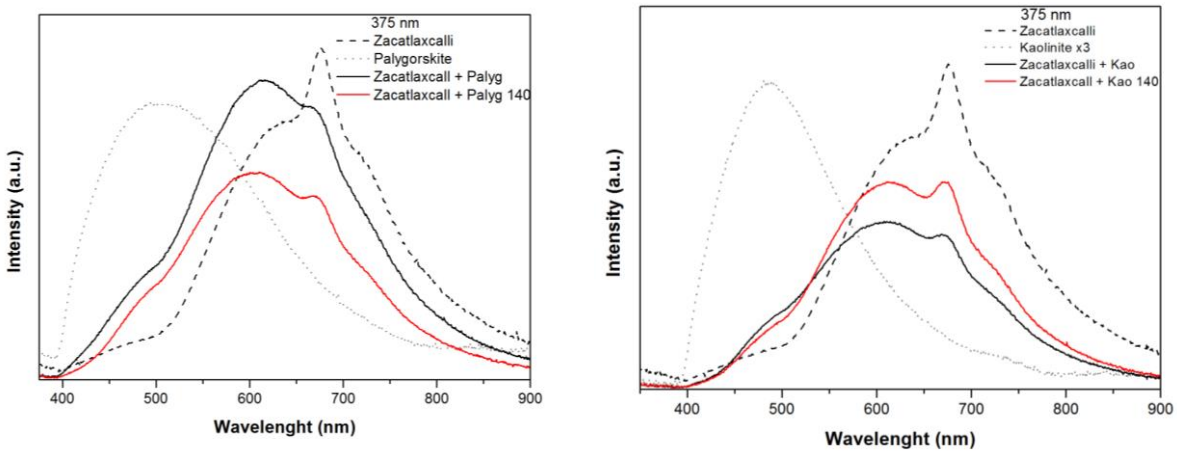

Fig. A.42 – Laser induced (λ_{exc}=375) emission spectra of Zacatlaxcalli@clays heated at 140ºC.

3.2.3. SERS

The '*' symbolizes the contribuition of the colloid.

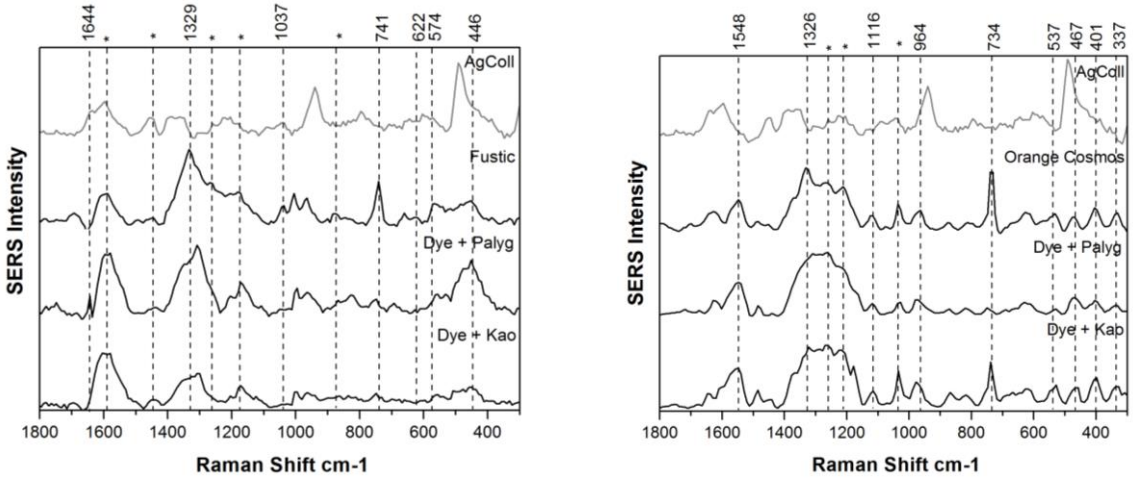

Fig. A.43 – SERS spectra of fustic and orange cosmos with both clays (λ_{exc}=785).

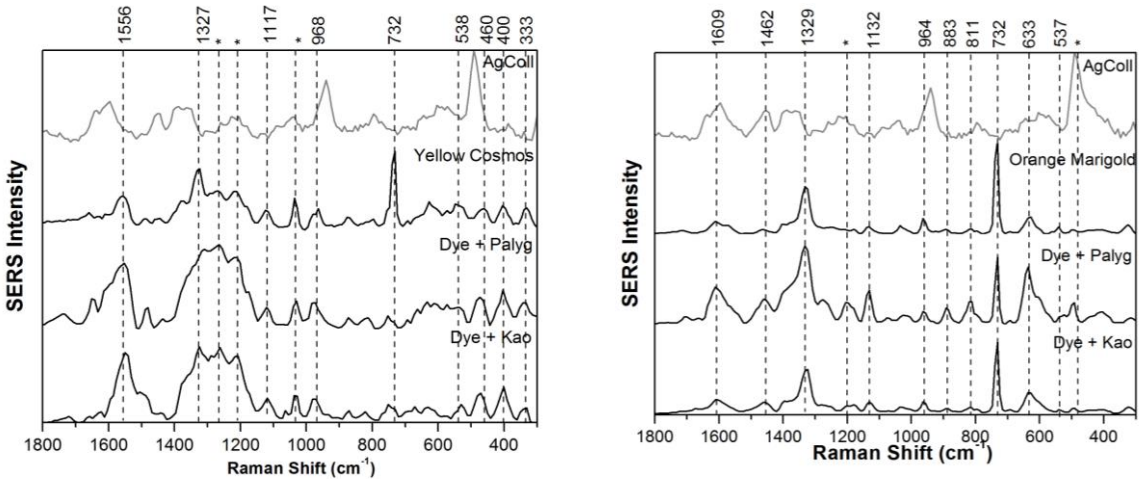

Fig. A.44 – SERS spectra of yellow cosmos and orange marigold with both clays (λ_{exc}=785).

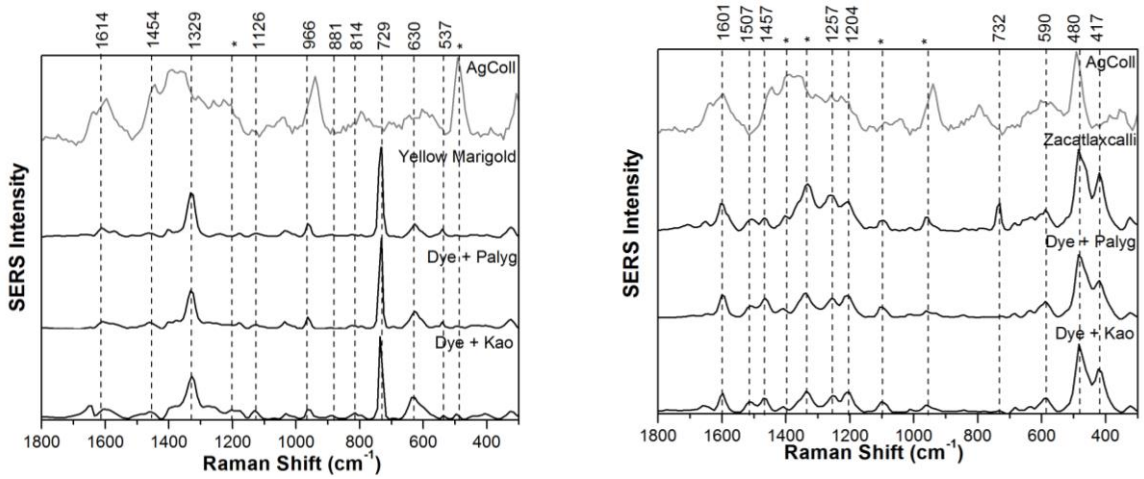

Fig. A.45 – SERS spectra of yellow marigold and zacatlaxcalli with both clays (λ_{exc}=785).

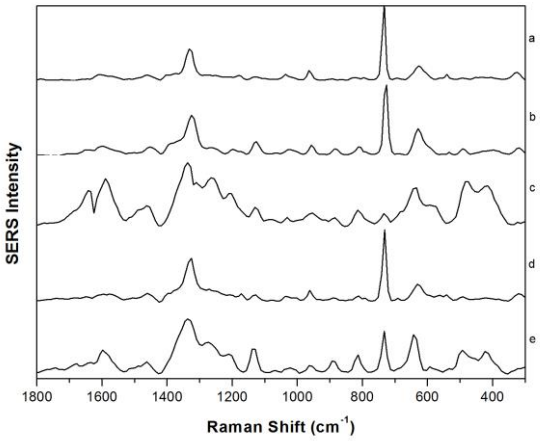

Fig. A.46 – SERS spectra of yellow marigold + palygorskite (a), dye@palygorskite heated at 140ºC (b), dye@palygorskite heated at 140ºC and washed (c), dye@palygorskite + water added during preparation (d), dye@palygorskite washed (e) (λ_{exc}=785).

Annex 4 – Photographs of the samples

4.1. Simplified Maya yellow replica

Table A.7 *– Photographs of the simplified Maya yellow replica samples recipe with and without heating (20% dye).*

Samples	Morin	Morin + Palyg	Morin + Kao	Annatto	Annatto + Palyg	Annatto + Kao
Unheated						
140ºC						
160ºC						
180ºC						
200ºC						
220ºC						

Table A.8 *– Photographs of the Annatto samples recipe with and without heating (50% dye).*

Samples	Annatto + Palygorskite	Annatto + Kaolinite
Unheated		
140ºC		
160ºC		

Annex 5 – Non-invasive characterization of the codices

Table A.9 *– Representation of all the known codices, provenance (area), group and conservation site.*

Group	Codex	Conservation site	Area
Maya	Dresden	Sächsische Landesbibliothek, Dresden	Maya
	Tro-Cortesianus	Museo de América, Madrid	
	Paris	Bibliothèque Nationale, Parigi	
	Grolier	Museo Nacional de Antropología, México City	
Borgia	Borgia	Biblioteca Vaticana, Roma	Oaxaca
	Laud	Bodleian Library, Oxford University, Oxford	
	Rios or Vaticano A	Biblioteca Vaticana, Roma	
	Vaticano B or 3773	Biblioteca Vaticana, Roma	
	Fejérváry-Mayer	Merseyside County Museum, Liverpool	
	Cospi	Biblioteca Universitaria, Bologna	
	Fonds Mexicanus 20	Bibliothéque Nationale, Paris	
Mixtech	Becker I	Museum Für Völkerkunde, Vienna	
	Becker II	Museum Für Völkerkunde, Vienna	
	Colombinus	Museo Nacional de Antropología, México City	
	Vindobonensis	National Bibliotek, Vienna	
	Selden	Bodleian Library, Oxford University, Oxford	
	Egerton	British Museum, London	
	Zouche-Nuttall	British Museum, London	

Table A.10 *– Representation of all the materials found in the non-invasive analysis performed in all codices [3].*

Color	Cospi	Zouche-Nuttall	Tro-Cortesianus	Fejérváry-Mayer
Binder	Proteinaceous	Proteinaceous	-	Proteinaceous
Ground	Gypsum	Gypsum + Calcium carbonate	Calcium carbonate	Gypsum + Anhydrite + Calcium carbonate
		Calcium carbonate		
Red	Cochineal	Cochineal	Hematite red + Kaolinite	Cochineal + clay
	Unknown dye			
Purple	-	Unknown dye	-	-

Blue	Maya blue + calcium carbonate	Maya blue + dolomite + calcium carbonate Maya blue	Maya blue	Maya blue + calcium carbonate
Grey	Carbon-based	Carbon-based	Maya blue	Carbon-based
Green	Indigo + unknown yellow dye + clay	Maya blue + orpiment	-	Maya blue + Orpiment Maya blue + Unknown yellow dye
Yellow	Orpiment Unknown dye + clay	Orpiment + calcium carbonate Unknown dye + clay	-	Orpiment
Orange	Unknown dye + clay	Unknown dye + clay Orpiment + cochineal (?) + Calcium carbonate	-	Unknown dye + clay
Brown	-	Unknown dye + clay	-	Unknown dye + clay Unknown dye
Black	Carbon-based	Carbon-based	Carbon-based	Carbon-based